Geochemistry, Geophysics, Geosystems

RESEARCH ARTICLE
10.1029/2020GC009565

Migration of Arc Magmatism Above Mantle Wedge Diapirs With Variable Sediment Contribution in the Aegean

A. Schaarschmidt[1], K. M. Haase[1], P. C. Voudouris[2], V. Melfos[3], and R. Klemd[1]

[1]GeoZentrum Nordbayern, Friedrich-Alexander Universität Erlangen-Nürnberg, Erlangen, Germany, [2]Faculty of Geology and Geoenvironment, National and Kapodistrian University of Athens, Athens, Greece, [3]Department of Mineralogy, Petrology and Economic Geology, Aristotle University of Thessaloniki, Thessaloniki, Greece

Key Points:

- Age-progression of magmatic centers reveals the linear migration of Aegean arc magmatism
- Subduction of heterogeneous continental lithosphere controls K-rich magma formation
- Sediment-rich mélange diapirs trigger arc magmatism at localized magmatic centers

Supporting Information:

Supporting Information may be found in the online version of this article.

Correspondence to:

A. Schaarschmidt,
anna.schaarschmidt@fau.de

Citation:

Schaarschmidt, A., Haase, K. M., Voudouris, P. C., Melfos, V., & Klemd, R. (2021). Migration of arc magmatism above mantle wedge diapirs with variable sediment contribution in the Aegean. *Geochemistry, Geophysics, Geosystems*, *22*, e2020GC009565. https://doi.org/10.1029/2020GC009565

Received 25 NOV 2020
Accepted 13 MAY 2021

Abstract Compiled data show the age progression of magmatic centers along the two approximately linear profiles from NE Greece and NW Turkey to the South Aegean Volcanic Arc. The age progression reveals the southwestward migration of arc magmatic activity from Oligocene to present, perpendicular to the Hellenic Trench. This is in accordance with the migration of the Aegean subduction zone due to the collision of oceanic and continental blocks, trench retreat, mantle flow, and coeval extension. We suggest that the subduction of large volumes of sediments and their contribution to the sub-arc magma source controlled the composition of calc-alkaline to high-K calc-alkaline and shoshonitic arc magmas during the past 30 Ma. The magma geochemistry and the approximately linear age-progressive migration of magmatic activity suggest focused ascent of mixed material from the subducted slab into the mantle wedge, most likely in the form of mélange diapirs. Geochemical data along the profile reveals increasing Sr and decreasing Nd isotopes during Upper Miocene in agreement with the ongoing subduction of continental blocks, low subduction rates, and development of an accretionary wedge. The different K-rich arc magmas reflect the variable subduction of sediments, whereas crustal assimilation often plays a minor role. Magmas with variable $^{87}Sr/^{86}Sr$, P/Nd, and Ba/La indicate a variable contribution of clastic, phosphate-bearing, and barite-bearing sediments. Low-degree partial melting in sediment-dominated mélange diapirs causes the formation of shoshonitic magmas with high Sr and P_2O_5 contents and high La/Yb in the northern Aegean.

Plain Language Summary The volcanic rocks of the South Aegean Islands were formed due to the subduction of the African plate below the Eurasian plate during the past 4 million years. Thirty million years ago, this subduction was situated further north and generated magmatic activity in northeast Greece and northwest Turkey. We present two profiles from the Northern Aegean to the South Aegean Islands across magmatic centers that document the temporal and spatial migration of the subduction zone from 30 million years ago to the present. A compilation of geochemical data of these magmatic rocks indicates that they were all generated by partial melting of the mantle above the descending plate, but this mantle source shows different compositions along the profile. Variable Sr isotope ratios as well as trace element concentrations of the magmas indicate that different sediments of the descending plate with variable amounts of clay, phosphate, or barite affected the mantle source of the magmas. The variable potassium and trace element concentrations of the magmas can be explained by the ascent of sediment and mantle material in heterogeneous balloon-like structures, so-called diapirs, above the descending plate.

1. Introduction

Subduction-associated plate boundaries are unstable and their location, structure, and morphology depend on factors such as rates of convergence and subduction, dip of the subducting slab, or subduction of volcanic chains or ridges (e.g., Cross & Pilger, 1982; Royden, 1993). The upper plate may be eroded, which leads to landward-directed migration of the arc magmatism away from the trench (e.g., Jicha & Kay, 2018). Alternatively, the subducting slab retreats which causes migration of the trench and the magmatic arc but also back-arc extension in the upper lithospheric plate (Faccenna et al., 2001). The Aegean region is an example where subduction migrated during the past ~90 million years due to the accretion of oceanic and

continental fragments leading to trench retreat and wide-spread extension in the overlying plate (e.g., Jolivet & Brun, 2010; Menant, Jolivet, et al., 2016; Royden & Faccenna, 2018). Numerous studies of the composition and genesis of Paleocene to recent magmatic rocks in the Aegean discuss the influence of individual tectonic processes like slab rollback, postcollisional extension, or slab tear in the Aegean and Anatolian region (e.g., Ersoy & Palmer, 2013; Marchev et al., 2004; Menant, Jolivet, et al., 2016). Other authors point out that subduction is more rapid than the convergence rate of the bounding African and Eurasian plates causing subduction orogeny in the eastern Mediterranean (Royden & Faccenna, 2018). Different models have been proposed to explain the formation of magmas erupting along volcanic arc fronts like the South Aegean Volcanic Arc (SAVA). Some models suggest hydrous flux melting of large portions of the hot mantle wedge that was infiltrated by aqueous fluids released from the subducting altered oceanic lithosphere (Cagnioncle et al., 2007; Iwamori, 1998; Tatsumi, 1986). Because of their low density, the melts rise in diapirs from the melting zone through the mantle wedge causing the formation of regularly spaced volcanoes in the arc front (Hall & Kincaid, 2001; Iwamori, 1998; Marsh & Carmichael, 1974). Alternative models of mantle wedge dynamics suggest diapiric ascent of (a) hydrated peridotite (Gerya & Yuen, 2003; Hasenclever et al., 2011; Nicholls & Ringwood, 1973), (b) subducted sediments (Behn et al., 2011), or (c) mixtures of peridotite with slab material (Marschall & Schumacher, 2012) into the melting zone beneath magmatic arcs. Structures consistent with diapirs connecting the slab and the arc front volcanoes are observed in seismic and magnetotelluric data at some subduction zones like that of Japan and western North America (McGary et al., 2014; Tamura et al., 2002). The volcanism in the SAVA is believed to be due to flux melting by the addition of hydrous fluids and melts to the mantle wedge (e.g., Francalanci & Zellmer, 2019). In contrast, much of the magmatism in the northern Aegean region is explained by postcollisional crustal or mantle melting possibly due to slab break-off and/or asthenospheric upwelling (e.g., Pe-Piper & Piper, 1992; Perkins et al., 2018). However, the composition of the northern Aegean magmatic rocks resembles that of the SAVA and thus some authors favor magma formation above the retreating slab (e.g., Innocenti et al., 1984).

Here, we compile geochronological and geochemical data of magmatic centers ranging in age from 33 Ma in the northern Aegean to recent at the active SAVA. We find that the magmatic centers form linear age-progressive trends perpendicular to the Hellenic Trench and argue that this reflects migration of arc magmatism due to consecutive diapir ascent from the retreating slab. The chemical and isotopic variation of the magmatic rocks indicates extensive mixing of mantle with subducted sediments within the diapirs with variable input of clastic sediment, phosphate, and barite. Our model suggests that this mixture melts to variable degree leading to the observed variation of calc-alkaline to shoshonitic magmas in the Aegean subduction zone.

2. Geotectonic Setting

The crust of the Aegean Microplate formed by accretionary processes of continental and oceanic units during the Cretaceous to Eocene. Most tectonic and seismological studies suggest that the subduction was continuous and formed one single connected slab (e.g., Wortel & Spakman, 2000), whereas Wei et al. (2019) present tomographic imaging of three slab segments possibly representing the Pindos, Tripolitza, and Ionian units below the western and northern Aegean. Trench retreat by some 600 km started ~45 Ma ago and caused wide-spread regional extension of the overriding lithosphere (Jolivet & Brun, 2010; Jolivet et al., 2013). The extension in the Aegean is NE-SW oriented (Figure 1a) and most of the present motion occurs close to the SAVA and in the fore-arc (Brun et al., 2016). After the closure of the Vardar ocean during the late Cretaceous the Pelagonian, Pindos, Gavrovo-Tripolitza, and Ionian Units were underthrusted and subducted beneath the Eurasian margin. Jolivet and Brun (2010) gave a detailed overview on the composition of these units within the Hellenides. The Ionian plate consists of Triassic to Cretaceous oceanic crust and up to 10 km of sediments, and is presently subducting beneath the SAVA (Pearce et al., 2012). Numerous magmatic intrusions and volcanic centers occur in the Aegean, and typically the magmatic rocks are calc-alkaline with varying enrichment of potassium up to shoshonitic compositions (Francalanci et al., 2005; Kirchenbaur et al., 2012; Pe-Piper et al., 2002). A decrease of the ages of the magmatic activity from NE to SW in the Aegean was noted previously, but has only been discussed as a general pattern (e.g., Agostini et al., 2010; Fytikas et al., 1984; Menant, Sternai, et al., 2016; Pe-Piper & Piper, 2006; Uzel et al., 2020).

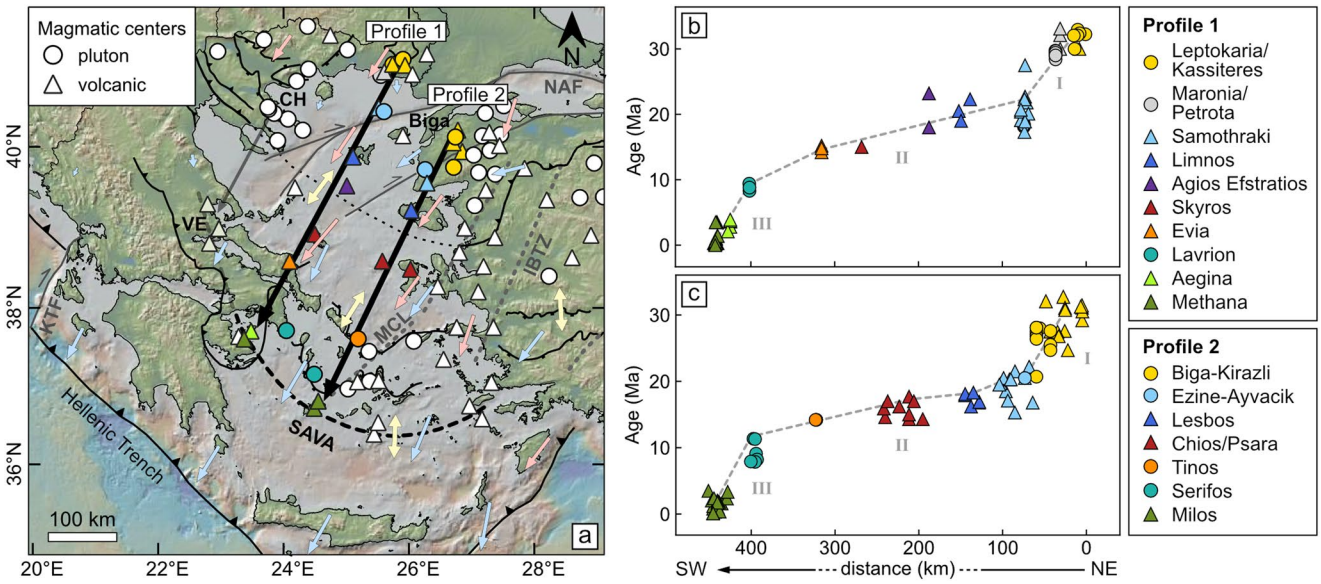

Figure 1. (a) Overview of the Aegean region with magmatic centers of Cenozoic age. Magmatic centers marked with color form the presented Profiles 1 and 2 (arrows) from the Northern Aegean to the South Aegean Volcanic Arc (SAVA). Blue arrows show the present-day plate motion relative to Eurasia, yellow arrows show the direction of extension (Flerit et al., 2004), and red arrows the direction of mantle flow indicated by mantle anisotropy (Brun & Sokoutis, 2010). (b, c) Age progression of magmatic activity along the profiles in (a). Arc magmatism migrated from NE (0 km) to SW (450 km) during the past 32 Ma. Ages based on published data (see Approach and Table S1). The uncertainty is below ±1.5 Ma for all locations. The numbers I, II, and III mark phases of different arc migration rates, that are discussed in the text. Biga, Biga peninsula; CH, Chalkidiki; IBTZ, İzmir–Balıkesir transfer zone; KTF, Kephalonia Transform Fault; MCL, Mid Cycladic Lineament; NAF, North Anatolian Fault; VE, Volos-Evia.

3. Approach

3.1. Geochronological Profiles

We compiled ages and compositional data for two profiles of magmatic centers from NE Greece and NW Turkey to the SAVA (Figure 1a) that lie perpendicular to the Hellenic Trench and parallel to the plate motion, the vector of extension, and the flow in the mantle wedge determined by seismic studies (Brun & Sokoutis, 2010; Jolivet et al., 2013; Menant, Sternai, et al., 2016; Paul et al., 2014). The compiled geochronological data reveals an age-progression of the magmatic activity from Oligocene to present along 450 km long, roughly straight profiles (Figures 1b and 1c). Both profiles show a similar age progression along parallel lines from 32 Ma-old rocks in the NE to the recent SAVA volcanoes of Methana and Milos (Figure 1). The ages of the magmatic activity overlap between many of the centers between 20 and 10 Ma, but there is a migration of the onset of activity by ~300 km. A potential third linear age-progressive profile further west reaches from Chalkidiki to the Volos-Evia area (Figure 1a). Although subduction in the Aegean reaches back to the Cretaceous, we start the profiles in the Oligocene because at that time continuous southward trench retreat and slab rollback started according to paleotectonic reconstructions (Menant, Jolivet, et al., 2016). Close spatial association of Eocene and Oligocene magmatic rocks in the Chalkidiki area, N Greece (Himmerkus et al., 2012; Jones et al., 1992) as well as in the Biga Peninsula, NW Turkey (Delaloye & Bingol, 2000; Yigit, 2012) indicate that magmatic activity was rather stationary at 55–35 Ma in the Northern Aegean. The voluminous Miocene magmatism in the Izmir-Menderes area, W Anatolia is not included in the profiles, because a slab tear beneath Anatolia caused complex processes of trench retreat and mantle flow (e.g., Brun & Sokoutis, 2010; Ersoy & Palmer, 2013). A NE-SW-directed migration of magmatic activity was observed in western Anatolia in the Miocene (Uzel et al., 2020).

3.2. Compilation of Geochemical Data

The magmatic centers along Profile 1 display a regular age progression of magmatic activity and are located at a central position of the Aegean subduction system. A data set of published major element, trace element, isotopic, and geochronological data from numerous studies allows us to investigate the geochemical

variation of the magmas along Profile 1 (Altherr & Siebel, 2002; Arikas & Voudouris, 1998; Baltatzis et al., 1992; Barbieri et al., 1998; Christofides et al., 2000; Del Moro et al., 1988; Elburg et al., 2018; Elburg & Smet, 2020; Eleftheriadis et al., 1994; Fytikas et al., 1979; Innocenti et al., 1981, 1984; Juteau et al., 1986; Kroll et al., 2002; Marchev et al., 1998; Matsuda et al., 1999; Mavroudchiev et al., 1993; Melfos et al., 2002; Mitropoulos et al., 1987; Papadopoulou et al., 2001, 2004; Pe-Piper, 1991; Pe-Piper & Piper, 1994, 2001, 2013; Pe-Piper et al., 1983, 2009; Perkins et al., 2018; Schaarschmidt et al., 2021; Seyitoğlu & Scott, 1992; Skarpelis et al., 2008; Stouraiti et al., 2010; Vlahou et al., 2006; Woelki et al., 2018). For the compilation of geochemical and geochronological data along Profile 2 further studies were considered (Aldanmaz et al., 2000; Altherr & Siebel, 2002; Altunkaynak & Genç, 2008; Baltatzis et al., 1992; Briqueu et al., 1986; Delaloye & Bingol, 2000; Ersoy et al., 2017; Fytikas et al., 1984, 1986; Iglseder et al., 2009; Innocenti et al., 1981; Juteau et al., 1986; Matsuda et al., 1999; Mitropoulos et al., 1987; Pe-Piper et al., 2009, 2014; Stouraiti et al., 2010, 2018; Uzel et al., 2020; Yigit, 2012). The compiled data set is attached in Table S1. Published data are complemented by new major element, trace element, Sr, and Nd isotope data of 12 plutonic and volcanic rocks from NE Greece and Limnos, measured at the GeoZentrum Nordbayern, Friedrich-Alexander Universität Erlangen-Nürnberg. The new data comprise three shoshonitic volcanic rocks from the Petrota graben and three calc-alkaline volcanic rocks from Kassiteres-Leptokaria in NE Greece, as well as three lavas from Limnos (Table S2). The descriptions of the analytical methods are presented in Text S1. The data set allows us to evaluate the petrogenesis and major geochemical variation during subduction and arc migration. The interpretations focus upon Profile 1 because it has the most complete data coverage.

4. Results

The selected magmatic centers including plutonic and volcanic rocks span two ~450 km long profiles between Leptokaria/Kassiteres and Methana (Profile 1) and between Biga-Kirazli and Milos (Profile 2, Figure 1). Profile 1 displays the following evolution of the magmatic activity. After Oligocene plutonism (33–30 Ma) and volcanism (33–27 Ma) in the area between Leptokaria and Maronia in NE-Greece ceased (Innocenti et al., 1984; Perkins et al., 2018; Schaarschmidt et al., 2021), magmatic activity started at Samothraki at ~23 Ma (Figure 1b) and remained active for ~7 million years (Christofides et al., 2000; Vlahou et al., 2006). The volcanic rocks of Limnos formed at 22–19 Ma and are followed by volcanic rocks at Agios Efstratios, Skyros, and Evia (Barbieri et al., 1998; Pe-Piper & Piper, 1994; Seyitoğlu & Scott, 1992). The 9 Ma old pluton at Lavrion (Skarpelis et al., 2008) fills the age gap between Evia and the young volcanic centers of Aegina and Methana in the SAVA (Elburg et al., 2018; Matsuda et al., 1999; Pe-Piper & Piper, 2013). Simultaneously to Oligocene magmatism in NE Greece magmatic activity occurred in the northern Biga Peninsula, NW Turkey, where Profile 2 starts with the Biga-Kirazli magmas (33–21 Ma) and continues southwestwards during Upper Miocene at Ezine-Ayvacik (22–15 Ma) in the Biga Peninsula (Aldanmaz et al., 2000; Altunkaynak & Genç, 2008; Delaloye & Bingol, 2000). Volcanism on the islands of Lesbos, Psara, and Chios was active from 18 to 14 Ma (Pe-Piper et al., 1994, 2014) and was followed by plutonism on Tinos at ~14 Ma (Altherr & Siebel, 2002; Bolhar et al., 2012; Stouraiti et al., 2010). Although Serifos is located 20 km off the profile, the plutonic activity on Serifos at 11–8 Ma (Iglseder et al., 2009) is included in Profile 2 since the island of Syros and Sifnos do not show any magmatic activity. Profile 2 ends at the island of Milos in the SAVA, where voluminous volcanic activity started at 3.5 Ma and lasted to historical times (Fytikas et al., 1986). Exposed plutonic rocks at Lavrion, Serifos, Tinos, Samothraki, Biga, and in NE-Greece represent intrusions at 3–10 km depth (Christofides et al., 2000) below active volcanoes at the time of emplacement. Most of the magmatic centers have diameters of <15 km and consist of lava flows and domes associated with shallow plutonic to subvolcanic rocks.

The magmatic centers along Profile 1 consist of plutonic and volcanic rocks with SiO_2 contents between 48 and 80 wt% and medium-K calc-alkaline to shoshonitic compositions (Figure 2a). The rocks from Maronia/Petrota, Samothraki, and Limnos are shoshonitic and mafic to intermediate samples show remarkably high P_2O_5 concentrations up to 1.0 wt% (Figure 2b) as well as high Sr, Th, and light rare earth element concentrations (Figure 3), whereas the other magmatic centers along the profile consist of calc-alkaline plutonic and volcanic rocks with lower trace element concentrations. All of the rocks have comparable patterns of incompatible elements with depletion of Nb and enrichment of fluid-mobile elements like Pb (Figures 3 and S1). The magmatic rocks of Profiles 1 and 2 show a large range of $^{87}Sr/^{86}Sr$ and $^{143}Nd/^{144}Nd$ from 0.704

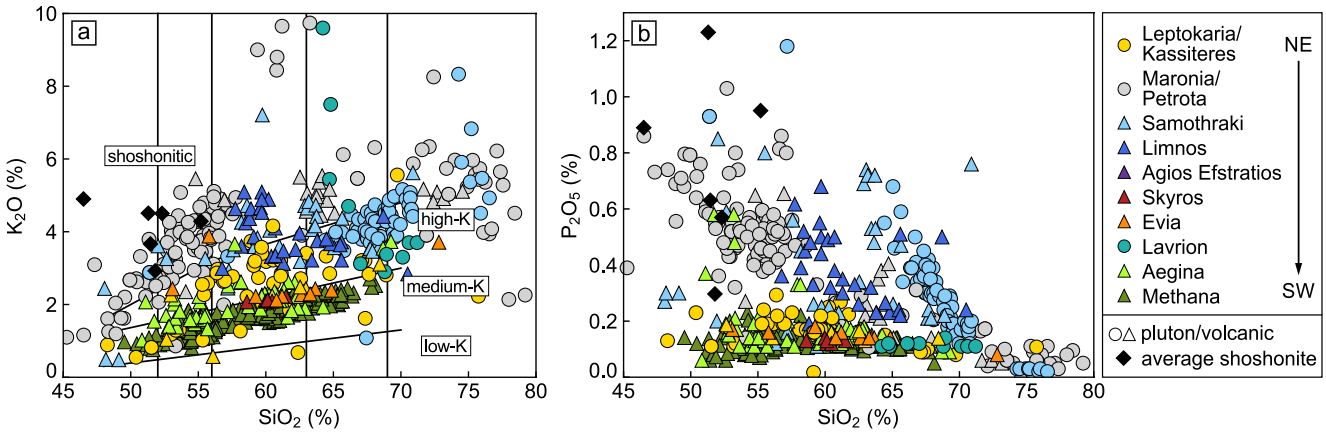

Figure 2. (a) SiO_2 versus K_2O plot of all magmatic rocks along Profile 1 shows shoshonitic compositions at Maronia, Samothraki, and Limnos and high-K to medium-K compositions at the other locations. Classification after Peccerillo and Taylor (1976). (b) SiO_2 versus P_2O_5 plot of all magmatic rocks along Profile 1 shows high P_2O_5 concentrations for mafic to intermediate rocks at Maronia, Samothraki, and Limnos. For comparison, average compositions of shoshonites from the following locations are shown: Vulcano and Stromboli, Aeolian Arc (Peccerillo et al., 2013), Tavua volcano, Fiji (Rogers & Setterfield, 1994), Kunlun Mountains, NW China (Zhang et al., 2008), Sunda Arc, and Mexican Arc (Schmidt & Jagoutz, 2017).

to 0.712 and from 0.5122 to 0.5128, respectively (Figure 4). Along Profile 1, the magmas at Samothraki (≤22 Ma), Limnos, Skyros, Evia, and Lavrion have the highest Sr isotope ratios. Some mafic to intermediate rocks with SiO_2 < 58 wt% at Samothraki, Limnos, and Evia show high $^{87}Sr/^{86}Sr$, comparable to their evolved endmembers (Figure 5a). The rocks at most locations like Maronia/Petrota, Samothraki, Limnos, and Evia have constant $^{87}Sr/^{86}Sr$ with increasing SiO_2, whereas Methana and Leptokaria/Kassiteres show increasing $^{87}Sr/^{86}Sr$ and decreasing $^{143}Nd/^{144}Nd$ with increasing SiO_2 (Figures 5a and 5c). The most mafic shoshonitic rocks of Maronia, Samothraki, and Limnos have higher La/Yb (Figures 5b, 6a, and 6b), Th/Yb (Figure 6f), and Nb/Yb (not shown) than the calc-alkaline rocks of the other centers.

5. Discussion

5.1. Magma Generation

The magmas of the active SAVA have been extensively studied and most authors agree that they were formed by hydrous melting of variably depleted mantle wedge that has been enriched by slab-derived components

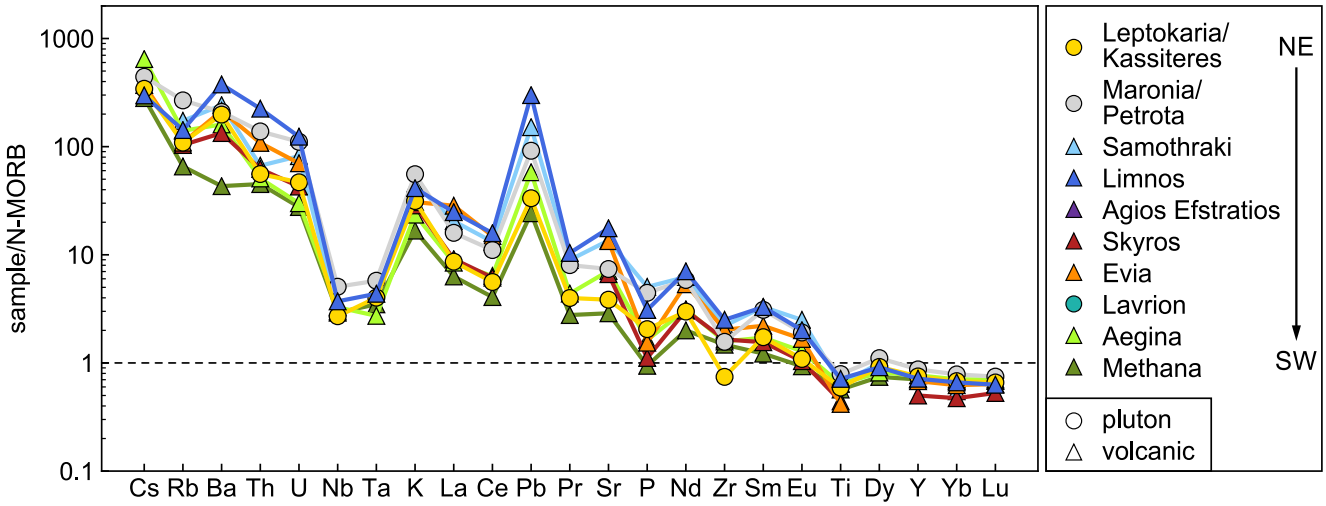

Figure 3. Incompatible element concentrations of representative mafic to intermediate samples (SiO_2 < 60 wt%) along Profile 1 normalized to N-MORB (Sun & McDonough, 1989) show a uniform signature for all magmatic rocks indicating a similar magma formation by partial melting of a mantle source that was enriched by slab-derived components from subducted sediments. The complete data set is shown in Figure S1.

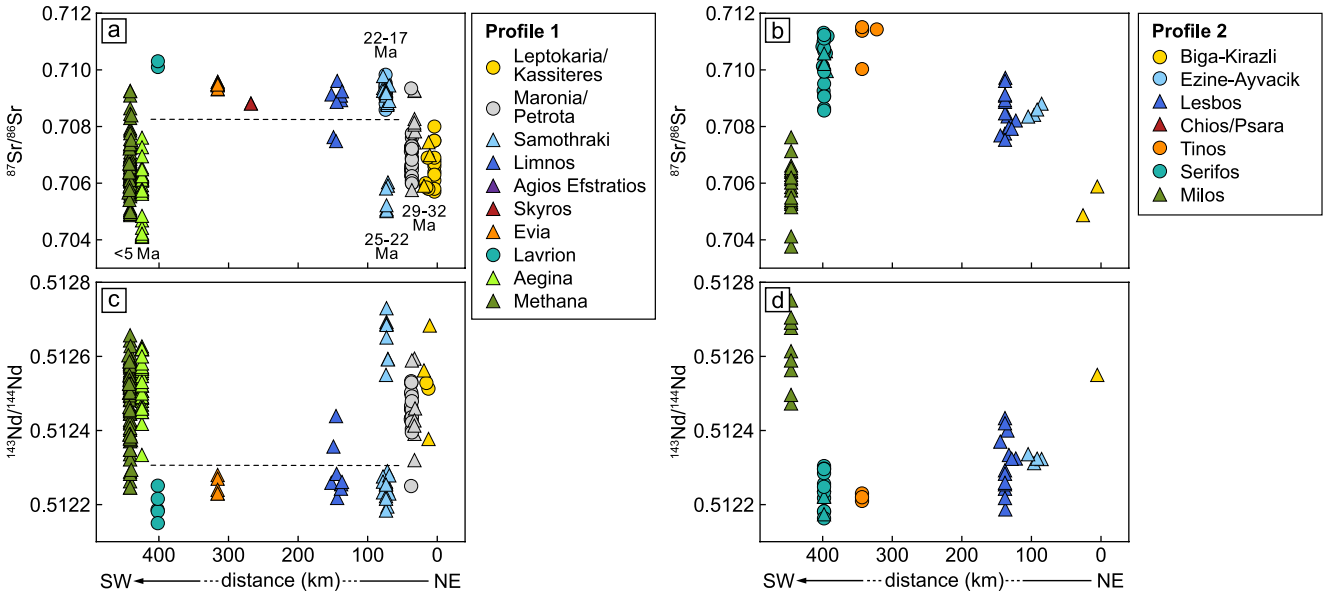

Figure 4. Variation of initial Sr and Nd isotope ratios along Profiles 1 (a, c) and 2 (b, d). (a) $^{87}Sr/^{86}Sr$ shows a step to more radiogenic compositions in the central part of Profile 1 at ages between 22 and 5 Ma. (b) $^{87}Sr/^{86}Sr$ along Profile 2 increases in two steps from NE to SW before decreasing again below 0.708 at the SAVA. (c, d) The Nd isotope ratios show opposite variations compared to the Sr isotopes along both profiles.

(Elburg et al., 2014; Francalanci et al., 2005). While the chemical variation of the mafic arc magmas mainly depends on the slab-mantle interaction, the composition of the evolved melts is affected by fractional crystallization, variable amounts of crustal assimilation, or magma mixing during ascent (e.g., Elburg et al., 2018). However, whereas it is generally suggested that magma generation at the SAVA is caused by flux melting in the mantle wedge in direct response to the active subduction, the formation of the older calc-alkaline rocks in the Aegean have been explained by other processes. For example, the formation of K-rich magmas is explained by post-collisional melting of metasomatized lithosphere by ascending asthenosphere (Biga Peninsula, Altunkaynak & Genç, 2008; Maronia, Perkins et al., 2018; Samothraki, Vlahou et al., 2006), by melting of underplated mafic lower crust by ascending asthenosphere (Limnos, Pe-Piper et al., 2009), or by decompression melting due to back-arc extension (Chios, Lesbos, Pe-Piper et al., 1994, 2014; Lavrion, Tinos, and Serifos, Stouraiti et al., 2010). Decompression melting of the asthenosphere in back-arcs typically yields MORB-like basalts, whereas close proximity to island arcs causes increasing input of slab components and flux melting (Pearce & Stern, 2006). No back-arc basalts are known from the Aegean but young alkaline basalts (that are not included in the presented profiles) occur in several back-arc regions of the Aegean and suggest decompression melting of asthenosphere with no or little metasomatism by a slab component (Aldanmaz et al., 2000; Marchev et al., 2004). Partial melting of metabasalts (e.g., garnet amphibolites) in the lower crust generates intermediate to felsic magmas (e.g., Qian & Hermann, 2013) unlike the basaltic to andesitic composition found in most Aegean magmatic centers. Finally, partial melting of lithospheric mantle beneath the Aegean by conduction from ascending asthenosphere is unlikely because the lithosphere-asthenosphere boundary beneath the Aegean (defined as the 1200°C isotherm) is unusually deep at 150–170 km (Sodoudi et al., 2006; Tesauro et al., 2009), that is, there is no evidence for thinning and melt production. Additionally, heating of the lithosphere would cause significant uplift (e.g., Roy et al., 2009) which is not observed in the western Aegean and rather, the magmatic rocks occur in basins. Thus, we suggest that these processes cannot explain the abundant mafic to intermediate magmatic activity in the Aegean. Rather, all magmas along the two profiles were generated by partial melting of the mantle wedge above the subducted slab because: (a) the magmatic activity follows the southwestward trench migration along continuous age-progressive profiles (Figure 1) implying a direct link to the slab rollback; (b) the trace elements show similar signatures with enrichment of fluid-mobile elements and depletion of Nb and Ta (Figure 3) for all magmatic centers indicating a variable slab contribution; (c) the incompatible element and isotope composition of Oligocene K-rich rocks in NE Greece closely resembles that of the active SAVA (Figures 3 and 4); (4) the abundance of mafic melts (<52 wt% SiO_2, in many cases as enclaves in felsic rocks,

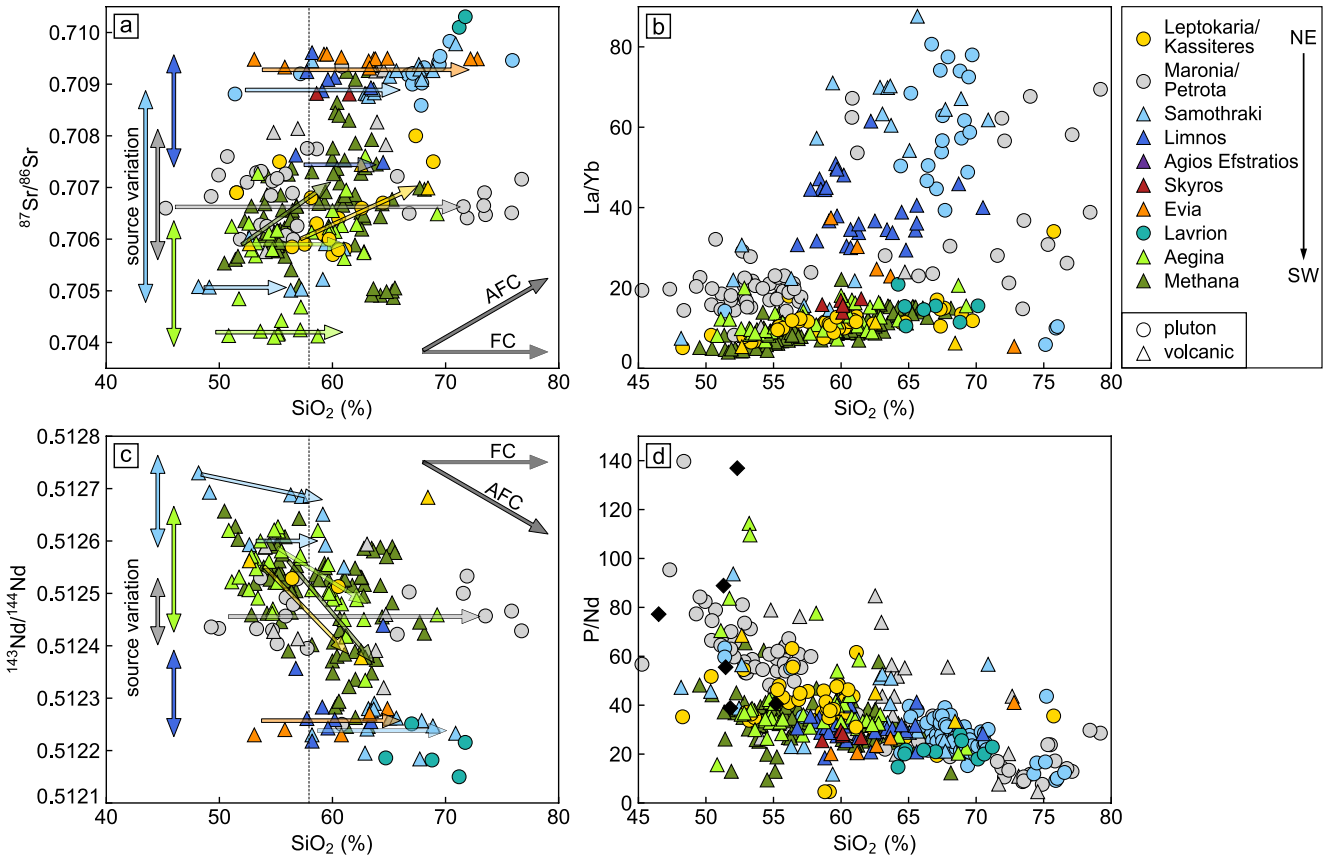

Figure 5. (a, c) Evolution of initial Sr and Nd isotopes with increasing SiO_2. Magmas with SiO_2 < 58 wt% (dashed line) indicate a relatively large isotopic variation of the mantle source at each magmatic center. (b) Higher La/Yb values in mafic to intermediate magmas at Maronia/Petrota, Samothraki, and Limnos indicate lower degrees of melting for the shoshonitic magmas. (d) P/Nd is not affected by the melting degree but the locations show significant variations indicating enrichment of the mantle by different sediments. For references of average shoshonite compositions, see caption of Figure 2.

Figure 2) along the line of magmatic centers implies that the parental magmas formed in the mantle wedge. Thus, we suggest that the age progression along the profiles across the Aegean reveals a continuous migration of the magmatic arc from NE to SW during the past 32 million years (Figure 1). The chemical variability of the magmas is controlled by the subduction of heterogenous continental and oceanic crust, which will be discussed in the following sections.

5.2. Variation of Magma Composition

The magma compositions change rapidly along Profile 1 and over small regional scales as exemplified in the change from the high-K calc-alkaline magmas of Leptokaria/Kassiteres (32.9–32.0 Ma) to the shoshonitic magmas at Maronia (29.8 Ma, Perkins et al., 2018). Similar changes between calc-alkaline and shoshonitic magmas occur on Limnos (Pe-Piper et al., 2009), and significant geochemical changes between magmatic centers are also known from the SAVA, for example, between Aegina and Methana (Elburg & Smet, 2020). The observed variation in the different magma types indicates variable magma sources, variable degrees of melting, and/or variable crustal assimilation. The mafic to intermediate rocks along Profile 1 show a large range of $^{87}Sr/^{86}Sr$ between 0.7040 and 0.7095 (Figure 5a). Since the magmas with <58 wt% SiO_2 were derived by partial melting of the mantle wedge with only minor effects of fractionation or assimilation, this approximately represents the isotopic range of the mantle source, which has been enriched by variable components of the subducted slab. Any crustal assimilation would lead to increasing SiO_2 and $^{87}Sr/^{86}Sr$, because the overriding continental crust consists of Mesozoic to Tertiary units,for example, widespread gneisses with $^{87}Sr/^{86}Sr$ > 0.710 (Buettner et al., 2005; Frei, 1995; McGrath et al., 2017). The relatively constant $^{87}Sr/^{86}Sr$ and $^{143}Nd/^{144}Nd$ between mafic and felsic rocks at Maronia, Samothraki, Limnos, and Evia

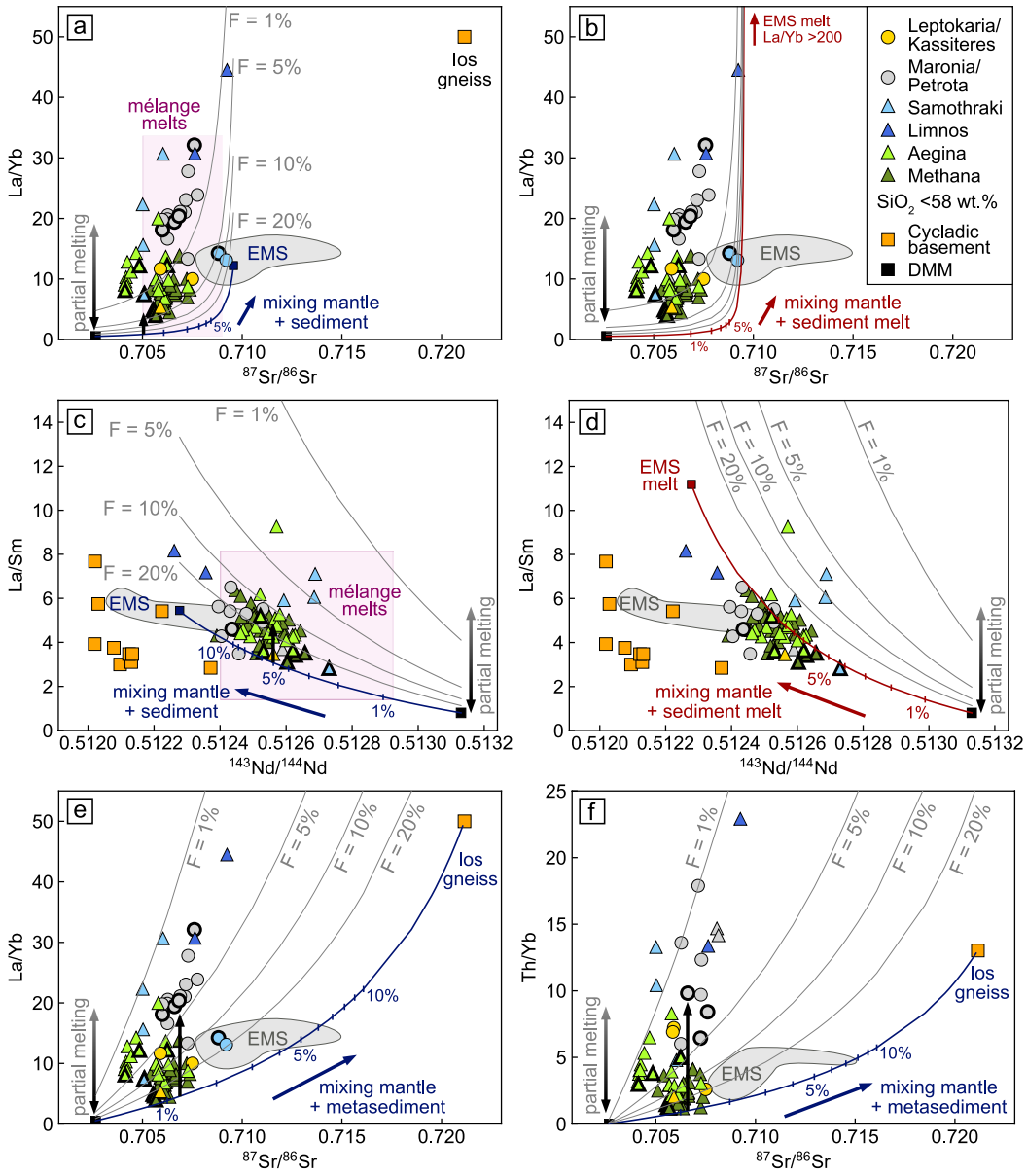

Figure 6. Modeling of $^{87}Sr/^{86}Sr$, $^{143}Nd/^{144}Nd$, and incompatible element ratios during mixing of depleted mantle (DMM) and slab-derived components and adjacent partial melting with variable degrees of melting (F). For modeling parameters see Text S2. Plotted data show magmas of Profile 1 with SiO_2 < 58 wt%. Mafic magmas with SiO_2 < 52 wt% are highlighted with bold rims. (a, c) The addition of Eastern Mediterranean Sediment (EMS) and partial melting could generate the La/Yb and La/Sm ratios of Methana magmas. The purple box represents the incompatible element ranges of experimental mélange melts (Cruz-Uribe et al., 2018) shown at isotopic ratios of metabasites from Cycladic ophiolitic mélanges (Bröcker et al., 2014; Stouraiti et al., 2017). (b, d) By contrast, mixing with EMS melt (Hermann & Rubatto, 2009) does not fit the data and gives unrealistic concentrations, for example, too high La/Sm ratios. (e, f) The addition of bulk metasediments like the Ios gneiss to the mantle wedge, together with lower melting degrees may explain the positive correlation of $^{87}Sr/^{86}Sr$ with La/Yb and Th/Yb in rocks from Maronia, Samothraki, and Limnos.

indicates that the evolution of these magmas is dominated by fractional crystallization (Figures 5a and 5c). By contrast, increasing $^{87}Sr/^{86}Sr$ and decreasing $^{143}Nd/^{144}Nd$ with fractionation at Aegina and Methana in the SAVA (Figures 5a and 5c) imply the influence of upper crustal contamination on the isotope composition of the evolved rocks (Elburg & Smet, 2020; Elburg et al., 2018). We conclude that in most cases the Sr and Nd isotope variation in mafic to intermediate rocks (<58 wt% SiO_2) reflects variable magma sources due to different recycling of slab components consisting largely of sediments.

The mafic to intermediate rocks from Evia and Samothraki or those from Leptokaria/Kassiteres and Maronia/Petrota have similar Sr isotope compositions but very different La/Yb (Figures 5a and 5b) suggesting different degrees of melting of similar sources (Schaarschmidt et al., 2021). Low degrees of melting lead, for example, to increased light rare earth element (REE) to heavy REE ratios (Figure 5b). Similar heavy REE contents relative to N-MORB of all studied magmas (Figure 3) indicate no influence of garnet in the magma source. Mafic to intermediate shoshonitic rocks at Maronia/Petrota and Samothraki show a stronger enrichment of most incompatible elements relative to heavy REE in comparison to the calc-alkaline rocks of the other magmatic centers (Figures 3 and 5b). This indicates lower degrees of melting in the NE part of Profile 1 between ~30 and 20 Ma. This is in accordance with formation models of potassic rocks by relatively low degree partial melting of a metasomatized mantle source (Condamine & Médard, 2014). However, some of these increased trace element concentrations can also indicate variable mantle depletion before subduction or enrichment of the mantle source by slab-derived components.

Mixing between the mantle and sedimentary material can occur either by an influx of sediment melts into peridotite causing partial melting, or by bulk mixing of peridotite with sediments followed by partial melting. To evaluate these processes we performed modeling of mixing and equilibrium melting of different endmember compositions using Sr and Nd isotope, La/Yb, La/Sm, and Th/Yb ratios, and compared the models to the magma compositions with SiO_2 < 58 wt% from Profile 1 (Figure 6). We show results of three different models where depleted mantle peridotite (DMM, Workman & Hart, 2005) is mixed with Eastern Mediterranean Sediment (EMS, Klaver et al., 2015) (Figures 6a and 6c), with EMS melt (melting at 900°C, 3.5 GPa, Hermann & Rubatto, 2009) (Figures 6b and 6d), and with Ios gneiss (Buettner et al., 2005) (Figures 6e and 6f), probably representing the subducted crustal material during Oligocene to Miocene, respectively. Following the binary mixing of the mantle with the three potential sediment components, the equilibrium melt compositions are calculated at variable melting degrees (F). For the detailed model parameters, see Text S2. The La/Yb, La/Sm, and Th/Yb ratios may be slightly affected by fractional crystallization that could increase these ratios by a factor of 2 from primary melt composition with 48–58 wt% SiO_2 content (Figure 5b). Thus, some samples would be shifted to lower ratios at primary melt composition, leading to higher estimated melting degrees than suggested by Figure 6. The models only give rough estimates of primary melt compositions, since the exact compositions of the Aegean mantle wedge and the slab-derived components, as well as the mineralogy of the mantle source during the past 30 million years are unknown. However, the modeling implies that the mantle was enriched by bulk sedimentary material (Figures 6a and 6c) rather than sediment melt (Figures 6b and 6d). Furthermore, enriched La/Yb and Th/Yb at Maronia, Samothraki, and Limnos are likely generated by lower melting degrees compared to Methana, as well as by mantle mixing with slab-derived sediment that has higher La/Yb, Th/Yb, and more radiogenic $^{87}Sr/^{86}Sr$ than EMS, similar to the Ios gneiss (Figure 6). The modeled $^{87}Sr/^{86}Sr$ versus La/Yb ratios (Figures 6a and 6b) strongly depend on the Sr concentration of the sediment component, because Sr-rich components such as the EMS will primarily influence the $^{87}Sr/^{86}Sr$ of the magma, leading to low La/Yb and low estimated melting degrees. Thus, the melting degrees of Aegean magmas in Figure 6a are probably underestimated, in case the subducted sediment has lower Sr concentrations than EMS.

Variable depletion of the mantle before slab-derived element enrichment, for example, higher La/Yb of the mantle source would also result in more enriched La/Yb ratios of mixed mantle partial melts. However, the positive correlation of La/Yb or Sm/Yb, as well as Nb/Yb with increasing $^{87}Sr/^{86}Sr$ and decreasing $^{143}Nd/^{144}Nd$ (Figure 6) indicates that the trace element ratios are controlled by variable addition of sediments, not by variable mantle sources. Due to the strong effect of sediments on the arc magma composition, the transfer of incompatible elements via aqueous fluids derived from subducted sediments or oceanic crust is negligible for the Aegean magmas, because the trace element concentrations of sediments and sediment melts are by a factor of >10 to >100 higher than that of slab-derived fluids (Hermann & Rubatto, 2009; Spandler et al., 2007). We conclude that the observed variation of the magma compositions along the profiles indicates mixing of peridotite with variable sediments (EMS to Ios gneiss) before partial melting.

The isotope and trace element modeling in Figure 6 shows that mixing of mantle with different bulk sediments and adjacent melting roughly reproduces the trace element pattern of the magmas along Profile 1. Similarly, the Nd/Sr compositions of the magmas along Profile 1 can be explained by the addition of bulk sediment with high Nd/Sr to the sub-arc mantle (Figure 7a), but not by the addition of sediment melts or

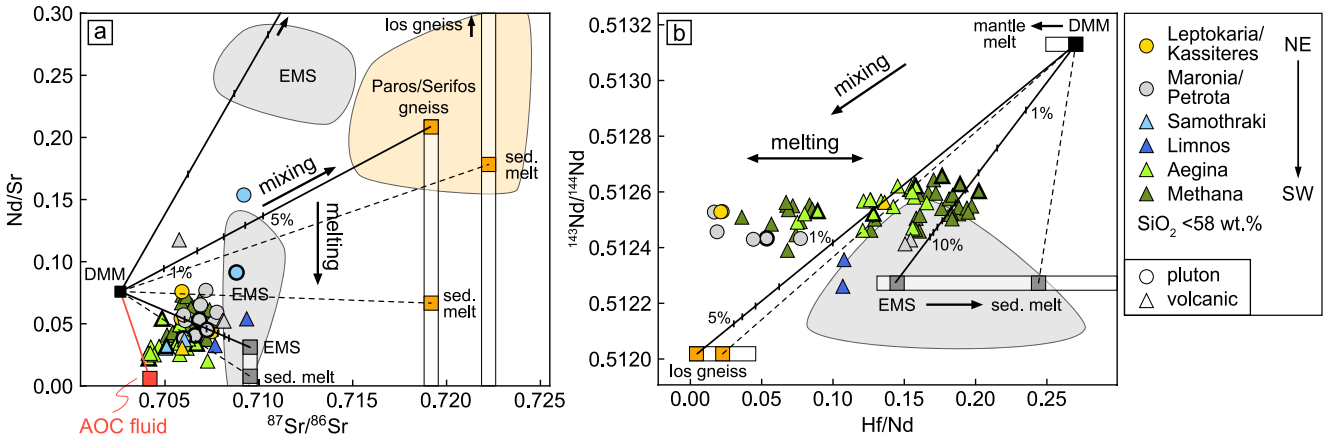

Figure 7. Isotope-incompatible element trends give insights into mixing and melting processes and may help to distinguish between mixing of mantle with fluids and sediment melts versus mixing of mantle with bulk sediment before melting (Nielsen & Marschall, 2017). The black lines indicate mixing of depleted mantle (DMM) with Ios gneiss, Paros/Serifos gneiss, and Eastern Mediterranean Sediment (EMS), whereas the dashed lines indicate addition of respective sediment melts. The sediment melt compositions are estimated using the experimental data of Hermann & Rubatto (2009), and the white bars represent the sediment melt composition at variable degrees of melting. The reddish line in (a) indicates addition of fluid derived from average altered oceanic crust (AOC fluid, Nielsen & Marschall, 2017). For modeling parameters see Text S2. (a) Increasing Nd/Sr with increasing $^{87}Sr/^{86}Sr$ can be explained by mixing of mantle with bulk sediments with high Nd/Sr, followed by melting, but not by mixing of mantle with sediment melts and fluids, because their Nd/Sr is much lower compared to bulk sediment (Hermann & Rubatto, 2009). (b) The magmas show variable Hf/Nd at relatively constant $^{143}Nd/^{144}Nd$, indicating mixing of mantle with bulk sediment before melting (Nielsen & Marschall, 2017). Experimental data indicate that melting of sediment mostly increases the Hf/Nd of the melt relative to the source (Hermann & Rubatto, 2009), whereas melting of peridotite slightly decreases the Hf/Nd of the melt (McDade et al., 2003).

fluids derived from the altered oceanic crust (Nielsen & Marschall, 2017), because these generate too low Nd/Sr of the magma source and the adjacent magmas in the Aegean. However, partial melting experiments of sediments and mélange rocks show variable results where some imply strong fractionation of Nd/Sr (Cruz-Uribe et al., 2018; Hermann & Rubatto, 2009), whereas other sediment melting experiments observed only minor Nd/Sr fractionation (Spandler et al., 2007). The Hf/Nd versus $^{143}Nd/^{144}Nd$ show a similar pattern (Figure 7b) that supports mixing of mantle with bulk sediments before melting, that generates variable Hf/Nd at similar $^{143}Nd/^{144}Nd$ (Nielsen & Marschall, 2017). By contrast, mixing of mantle with, for example, EMS melt would generate relatively high Hf/Nd of the magma source, that does not overlap with the magmas along Profile 1 (Figure 7b). Experimental studies suggested that melts of mélange-hybridized mantle resemble primitive arc melts (Codillo et al., 2018; Cruz-Uribe et al., 2018), and their La/Yb and La/Sm ratios overlap with those of the Aegean magmas (Figures 6a and 6c), but these experimental melts have too low FeO^T and also the Ba, Sr, and Ce concentrations are lower than in the Aegean magmatic rocks. In contrast to global oceanic arc magmas (Nielsen & Marschall, 2017), the Aegean magmas show a larger isotopic variation of the magma source (Figures 5a and 5c), that partly correlates with enriched trace element ratios (Figures 6 and 7). Given the very heterogeneous and unknown composition of the subducting sediments, the sediment volume, and the water content, we believe that most of the geochemical signatures of the Aegean arc magmas can be explained by mélange melting. For example, the relatively high Ba/La ratios of some Aegean arc magmas probably indicate that portions of the subducted sediments contain barite as suggested for some lavas from Aegina (Elburg & Smet, 2020). We propose that variable degrees of partial melting of a heterogeneous peridotite-sediment mélange explain the close spatial and temporal association of high-K calc-alkaline and shoshonitic rocks, for example, at Maronia-Kassiteres, Limnos, or Lesbos.

5.3. Evidence for Changes of Subducted Sedimentary Material

The Sr, Nd, and Pb isotopic composition of mafic SAVA magmas reflects the addition of a slab-derived sediment component to a variably depleted mantle source (e.g., Francalanci et al., 2005; Klaver et al., 2015, 2016; Woelki et al., 2018). Previous models used EMS as subducted sediment component during recent subduction along the Hellenic trench (Klaver et al., 2015). However, the composition of the subducted sediments can change on short time scales and, for example, Elburg and Smet (2020) found evidence for the subduction of sediments with variable barite contents that caused significant variation of Ba/Th and Ba/La

in the lavas of Aegina. The variation of $^{87}Sr/^{86}Sr$ of mafic to intermediate magmas with time along Profile 1 (Figure 4a) indicates variable input of slab-derived sedimentary or other crustal material to the mantle wedge. Although large crustal portions of the continental Gavrovo-Tripolitza, the Phyllite-Quartzite, and the Ionian unit were accreted between 35 and 15 Ma, most of these blocks were subducted (e.g., Jolivet & Brun, 2010) and provide a range of different crustal lithologies that potentially affected the sub-arc mantle. The upper crust of these continental blocks consists mainly of Mesozoic to Tertiary sedimentary sequences ranging from pelitic to volcaniclastic, platform, and flysch sediments. Accreted parts of the lower crust crop out in the metamorphic core complexes of the Cyclades, for example, the gneisses and metasediments at Paros, Serifos, and Ios (Buettner et al., 2005; McGrath et al., 2017). We suggest that the variation in Sr and Nd isotope ratios (Figure 4) reflect the changes of amount and type of subducting sedimentary material with time, similar to observations in calc-alkaline to shoshonitic lavas of the Sunda-Banda arc (Elburg et al., 2004). Variable sedimentary fluxes into trenches of subduction zones were also shown to correlate with the K, Ba, Sr, and Th concentrations of arc magmas (Plank & Langmuir, 1993), and thus the high K concentrations of Aegean magmas can also be related to variable input of subducted sediment.

Slab-derived components like aqueous fluids, hydrous melts, or mélange diapirs affected the trace element and isotopic composition of the mantle wedge, which is supported by the enriched large-ion lithophile elements (LILEs) and depleted high field strength elements (HFSEs) in all magmas along the profiles (Figure 3). The variation of $^{87}Sr/^{86}Sr$ in the Aegean magmatic rocks reveals a major change of the amount or type of subducted material at about 22 Ma, where the Sr isotopic ratio shifts toward high values between 0.7085 and 0.7100 (Figure 4a). The $^{87}Sr/^{86}Sr$ of carbonate sediments ranges between 0.7078 and 0.7090 for all Phanerozoic carbonates (Burke et al., 1982) and therefore cannot have caused the high $^{87}Sr/^{86}Sr > 0.709$ in the volcanic and plutonic rocks. The crustal material that enriched the mantle source between 22 and 5 Ma must have been rather dominated by continent-derived clastic sediments with $^{87}Sr/^{86}Sr$ of >0.710. This increase of subducting continental material coincides with the development of a thick accretionary wedge 23 Ma ago and the exhumation of high-pressure units from the subduction channel (Jolivet et al., 2013), whereby both processes support an increase in sediment subduction. In contrast, the $^{87}Sr/^{86}Sr$ in magmatic rocks from NE Greece and the SAVA is lower and more variable, suggesting that smaller volumes and/or different sediments contributed to their magma source. Figures 6e and 6f show that the high La/Yb and Th/Yb ratios at Maronia, Samothraki, and Limnos require the addition of a slab-derived component with high La/Yb and Th/Yb ratios like the Ios gneiss, which represents the subducted crust during Oligocene to Miocene and therefore is a suitable end-member for this model. We suggest that the strong increase of $^{87}Sr/^{86}Sr$ in the magmas during the Miocene is caused by increasing amounts of slab-derived sedimentary contribution to the mantle source at low subduction rates, which will be discussed below.

Trace element ratios like Nd/Sr, Ba/La, and P/Nd, which are not strongly affected by the melting degree, also show significant variations in magmas with $SiO_2 < 58$ wt% along Profile 1 (Figure 8). These variations probably also indicate changes in subducted sediment composition. High P_2O_5 concentrations in intermediate Samothraki and Limnos magmas indicate that no significant apatite fractionation occurred during their earlier evolution and high P contents in the primary mantle-derived melts. Fractional crystallization of the magmas leads to decreasing P/Nd (Figure 5d) and Ba/La values but we find that the mafic to intermediate magmas from Maronia, Kassiteres, and Aegina show higher P/Nd and Ba/La than the Methana lavas without a significant correlation with Sr isotopes (Figures 8a and 8b). Elburg and Smet (2020) suggested that high Ba/Th (analogous to high Ba/La) ratios of some Aegina lavas reflect the subduction of barite-rich sediments, which may also explain the Ba enrichment in Kassiteres and Maronia rocks in NE Greece with Ba/La >30 (Figure 8a). Element enrichment via aqueous fluids would also lead to increasing Ba/La ratios, but at the same time to decreasing Ba/Rb (Elburg & Smet, 2020; Spandler et al., 2007), which is not observed in the Maronia, Kassiteres, and Aegina magmas (Figure 8c). By contrast, high Ba/La ratios mostly coincide with high Ba/Rb ratios, which indicates enrichment of Ba relative to the other LILE in mafic to intermediate magmas. The presence of clay minerals, micas, or amphibole in the magma source leads to elevated LILE of arc magmas, but only barite can strongly fractionate Ba from the other LILE. Thus, high Ba/La and Ba/Rb at Maronia, Kassiteres, and Aegina support the subduction of contribution of barite-rich sediments (Figure 8c).

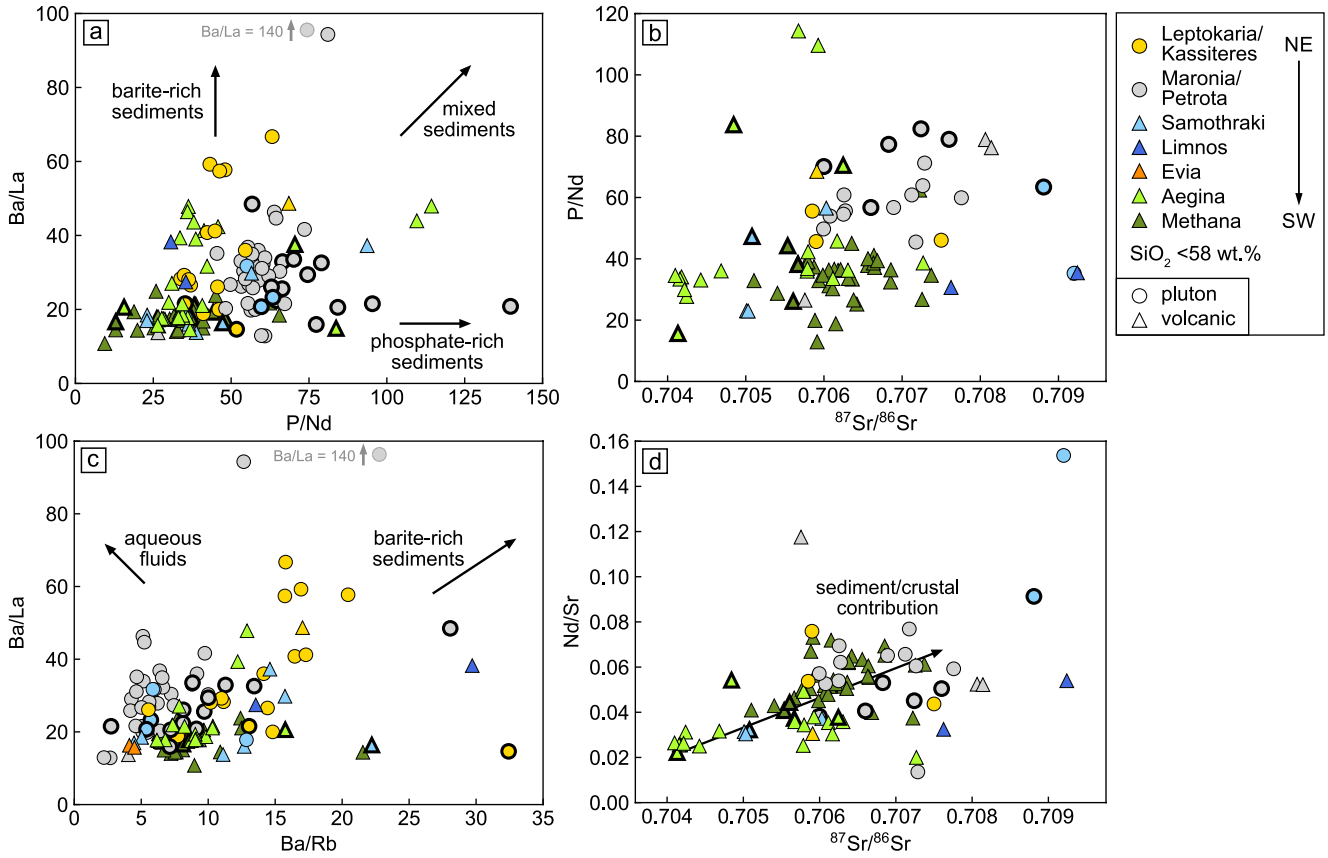

Figure 8. The P/Nd, Ba/La, Ba/Rb, and Nd/Sr ratios of magmas with SiO_2 < 58 wt% reflect compositional variations of the mantle source due to enrichment by different slab-derived sedimentary components. Mafic magmas with SiO_2 < 52 wt% are highlighted with bold rims. (a) High P/Nd and Ba/La indicate contribution of phosphate-bearing and barite-bearing sediments at Maronia, Kassiteres, and Aegina. (b) Initial Sr isotopes versus P/Nd shows no clear positive correlation, but high P/Nd ratios at Maronia and Aegina imply the contribution of P-rich sediments. (c) Positive correlation of Ba/La with Ba/Rb ratios supports Ba enrichment by barite-rich sediments, but not by slab-derived fluids. (d) Initial Sr isotopes show a positive correlation with the Nd/Sr ratios along Profile 1, which indicates the contribution of a slab-derived sediment component (see also Figure 7a) or crustal assimilation.

Several mafic to intermediate magmas at Maronia, Samothraki, and Aegina show P/Nd ratios >60 that are higher than the P/Nd in respective rocks from Leptokaria/Kassiteres or Methana in the SAVA (Figures 5d and 8a). At pressures between 1 and 3 GPa, the bulk P content of the subducted crust is stored in apatite and will be consumed rapidly by a coexisting melt (Konzett & Frost, 2009). The generally elevated P_2O_5 concentrations in global subduction-related shoshonites, for example, from Fiji (Rogers & Setterfield, 1994) or the Sunda Arc (Schmidt & Jagoutz, 2017) may be controlled by lower melting degrees and/or higher apatite solubilities in alkaline melts compared to calc-alkaline magmas. However, global shoshonites show extremely variable P_2O_5 between 0.3 and >1.0 wt% (Figure 2b), as well as variable P/Nd (Figure 5d), that are not only related to higher solubilities or low degrees of partial melting, but also requires variable P_2O_5 contents of the magma source. Thus, the high P_2O_5 and P/Nd in magmas from Maronia, Samothraki, and Aegina reflect either subducted P-rich sediments or an enrichment of P by fluids from the subducted slab. However, an efficient transport of P and HFSE by hydrous fluids is disputed (Gao et al., 2007) and rather, the variable P/Nd is thought to indicate compositional variations of the subducted sediments with time (Schaarschmidt et al., 2021). Phosphate-rich sediments may have been subducted together with clastic sediments and contributed to the arc magma formation via sediment melts or mélange diapirs. Phosphate enrichment is observed in pelagic sediments during times of high productivity and P_2O_5 contents up to 3 wt% are known from Pacific red clays (Plank & Langmuir, 1998), but P/Nd of these sediments is around 30. However, pelagic black shales of Jurassic and Cretaceous age were deposited in the deeper basins of the western Tethys (Emeis & Weissert, 2009) and sapropels of Pliocene and Pleistocene age with P_2O_5 contents up to 0.5 wt% occur in the eastern Mediterranean (Wehausen & Brumsack, 1999) and such sediments were

probably subducted. Shallow marine sediments with 20–30 wt% P_2O_5 were deposited during Upper Cretaceous to Eocene times along the margins of the Tethys and today form major phosphorite resources in the Mediterranean region (Abed, 2013; Notholt, 1985). The P/Nd ratios of phosphorites from Egypt range between 700 and 4,500 (Imamoglu et al., 2009) and a small contribution of phosphate in the bulk subducted sediment would be sufficient to increase the P/Nd of the magma source. We suggest that increased P_2O_5 contents and P/Nd ratios in the shoshonitic magmas in the Aegean reflect the subduction of units that contain phosphate-bearing sediments.

It was previously suggested that low Nd/Sr of mafic arc magmas indicate the contribution of partial melts from subducted carbonate sediments (e.g., Aiuppa et al., 2017). Melting experiments on pelitic sediments have shown that the Nd/Sr ratio is fractionated during partial melting, resulting in much lower Nd/Sr ratios for sediment melts compared to bulk sediment (Hermann & Rubatto, 2009). The magmas along Profile 1 show a positive correlation between $^{87}Sr/^{86}Sr$ and Nd/Sr with Samothraki rocks having the highest Sr isotope and Nd/Sr ratios (Figure 8d). This can be caused by assimilation of crustal material, which is likely for Methana, or by the addition of a slab-derived sediment component with high Nd/Sr. The Nd/Sr and Sr isotope ratios are higher than those of carbonate and thus, Nd/Sr in the Aegean magmas does not reflect variable carbonate subduction. Rather, the slab-derived components affecting the sub-arc mantle may have been similar to, for example, bulk EMS for the active arc, or metasediments like the gneisses of Serifos/Paros, that may represent the subducted continental crust during Oligocene to Miocene (Figure 7a). We conclude that much of the isotope and trace element variation of the magmas along Profile 1 is due to the variable volume and composition of the subducted sedimentary material. This is in accordance with the heterogeneous constitution of the subducted plate during the past 30 million years proposed by tectonic models (e.g., Jolivet & Brun, 2010).

5.4. Arc Magmatism Triggered by Mantle Wedge Diapirs

The incompatible element and isotopic signature of arc magmas imply element transfer from the subducted slab to the sub-arc mantle wedge. In some models, the ascent of hydrous fluids from the subducted altered oceanic lithosphere to the mantle wedge causes flux melting of peridotite over large regions (Iwamori, 1998; Spiegelman & McKenzie, 1987) and these melts may rise as diapirs (e.g., Tatsumi, 1986). The Hellenic Trench contains sediments with a thickness of 8 km and 109 km^3/million years of this sediment is subducted (Clift & Vannucchi, 2004; Kopf, 2003). Additionally, sediments and continental crustal portions of similar thickness were likely subducted in the past 30 million years, causing the enriched incompatible element composition (Figure 3) and high $^{87}Sr/^{86}Sr$ and low $^{143}Nd/^{144}Nd$ isotope ratios of the Aegean magmatic rocks (Figures 7 and 8). Thus, the slab component affecting the magma source was dominated by the sediment rather than by a hydrous fluid from altered basalt. Fluid dynamic models suggest that thick layers of subducting sediments like those in the Aegean form diapirs above the slab due to the lower density of sediment compared to the dry mantle (Behn et al., 2011; Menant, Sternai, et al., 2016). Depending on the sediment thickness and the thermal structure of the mantle wedge, mélange diapirs consisting of mixed mantle rocks and slab components may ascend from the surface of the subducted plate into the mantle wedge, where higher temperatures and decompression lead to partial melting of the mélange (Marschall & Schumacher, 2012). The abundance of high-pressure mélange rocks on the Cycladic Islands (e.g., Bulle et al., 2010) suggests that mélange formation is a common process along the subducting Hellenic slab.

The regular spacing of the magmatic centers along Profiles 1 and 2 with typical diameters of <20 km reflects localized magma pulses causing magmatic activity for <5 million years at each magmatic center (Figure 1). Up to ten magmatic centers formed over a period of 32 million years with approximately constant lateral spacing above the retreating subducting slab suggesting that diapirs rise from the same depth and location of the retreating slab. Numerical models indicate that disturbances on the boundary layer may cause the formation of a new diapir (Hasenclever et al., 2011). Alternatively, the structure of the slab such as the presence of fracture zones (Manea et al., 2014) may determine the location of diapiric instabilities and seismic studies of the subducting slab beneath the Aegean recorded numerous fracture zones perpendicular to the arc (Sachpazi et al., 2016). The geochemical variations in the Aegean magmatic rocks suggest that mixing of sediments with peridotite occurred before melting (Figures 6 and 7), implying that the diapirs probably consist of a mélange of the source rocks that rise from the slab surface and melt in the hot shallow mantle

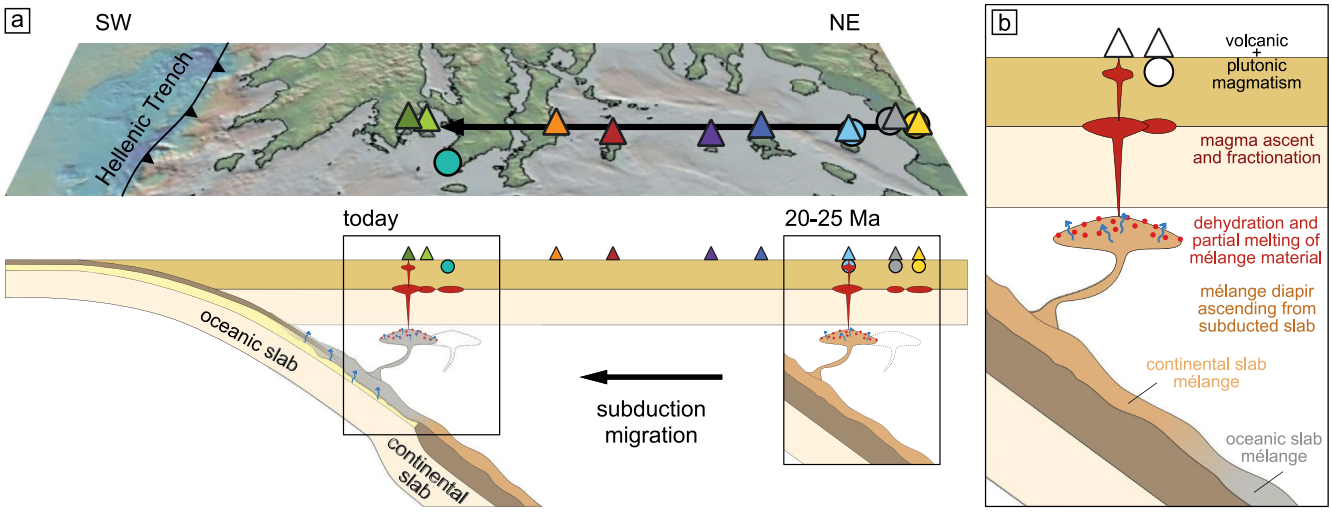

Figure 9. Suggested model of arc magmatism above mélange diapirs leading to the formation of the age-progressive line of magmatic centers due to subduction migration from Oligocene to present. (a) Profile 1 from NE Greece to the Hellenic Trench with schematic subduction model. (b) Sediment-rich mélange diapirs ascend from the subducted slab into the mantle wedge and dehydration leads to partial melting and arc magmatism (after Marschall & Schumacher, 2012). The constitution of the subducted slab (oceanic or continental) controls the geochemical composition of the arc magmas.

(Figure 9) above a constant slab depth of 90–100 km (Halpaap et al., 2018). Seismic profiles close to Methana in the SAVA were interpreted to show a localized ascent of fluids or melts from the slab into the mantle wedge (Halpaap et al., 2018), but the Vp/Vs anomalies could also represent hydrated rocks in the mantle wedge (Karakonstantis et al., 2019). Thus, we suggest that diapirs connected to the gravitationally instable subduction channel on the retreating slab caused the regularly spaced age-progressive arc magmatism between the northern Aegean and the SAVA in the past 32 million years (Figure 9).

5.5. Arc Migration in the Course of Aegean Tectonics

One exceptional feature of the complex tectonic history of the Aegean is the alternating subduction of oceanic and continental lithosphere since the Cretaceous as indicated by the presence of low-velocity anomalies of >2,000 km long subducted slab in the upper and lower mantle (Jolivet & Brun, 2010; van Hinsbergen et al., 2005). After the closure of the Pindos Ocean at ~35 Ma subduction of continental crust of the Gavrovo-Tripolitza and the Ionian units set in and changed back to subduction of oceanic crust of the Mediterranean Ocean at ~14 Ma in the central Aegean (Figure 10, Menant, Jolivet, et al., 2016). The subduction of continental lithospheric units significantly affected the subduction rate leading to decreasing rates from

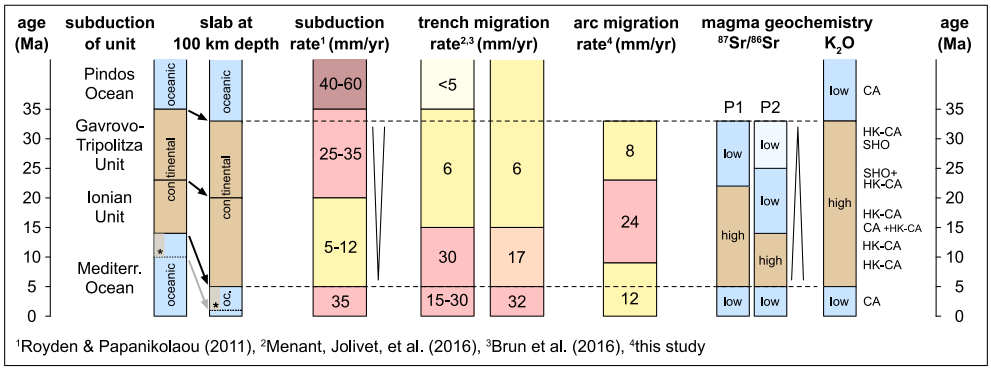

Figure 10. Time chart displaying the tectonic and geochemical characteristics of the Aegean subduction system and related arc magmatism. The subducted slab material at sub-arc depth was estimated using the subduction rates of Royden & Papanikolaou (2011). Subduction of continental crust in the VE area lasted longer until 10 Ma (marked with *). P1 = Profile 1, P2 = Profile 2, CA = calc-alkaline, HK = high-K, SHO = shoshonitic.

>40 mm/yr during late Eocene to ~10 mm/yr during late Miocene, followed by increasing subduction rates up to 35 mm/yr in recent times (Figure 10, Royden & Papanikolaou, 2011). The partly collision, partly subduction of continental fragments led to southwestward trench retreat with trench migration rates around 6 mm/yr until Middle Miocene and increasing rates until present (Figure 10, Brun et al., 2016; Menant, Jolivet, et al., 2016). The velocity of arc migration along the profile can be estimated using the ages of the magmatic rocks and the present distances between the magmatic centers (Figure 1b), although these may be affected by extension. Thus, the arc migration can be divided into (a) a slow arc migration of 8 mm/yr until 23 Ma, (b) an increased migration rate of 24 mm/yr until 9 Ma, and (c) a slow rate of 12 mm/yr from 9 Ma to present (Figures 1 and 10). The observed arc migration rates do not correlate with the trench migration rates and reflect the complex interplay of subduction rate, trench retreat, slab buoyancy, and overriding plate kinematics. The slow rate displayed by the youngest volcanic centers may be due to the fact that the most recent extension occurs in the fore-arc (Brun et al., 2016).

Some of the geochemical variation from Eocene to present can be correlated with the tectonic evolution of the Aegean. We suggest that the occurrence of high-K and shoshonitic magmas between 33 and 5 Ma reflects the subduction of continental lithosphere, whereas Eocene and Pliocene-Quaternary calc-alkaline magmas display subduction of oceanic crust with up to 8 km thick sediments (Figures 9 and 10). Increasing $^{87}Sr/^{86}Sr$ and decreasing $^{143}Nd/^{144}Nd$ from Oligocene to late Miocene (Figure 4) may be correlated with decreasing subduction rates and/or underthrusting of the Gavrovo-Tripolitza continental unit causing a massive increase of sediment subduction (Figure 10). Subduction of the Ionian platform at very low subduction rates coincides with I-type and S-type plutonism in the Cyclades at 14–8 Ma. These magmas show the highest $^{87}Sr/^{86}Sr$ >0.7010 along the two profiles (Figure 4), indicating the largest contribution of crustal material by assimilation, but probably also in the magma source. Low subduction rates may enable the contribution of larger rock volumes to the formation of mélange diapirs, thus a stronger sedimentary contribution to the sub-arc mantle source.

5.6. The Volos-Evia Volcanics as Prolongation of the SAVA

The high-K calc-alkaline lavas of the Volos-Evia area (Figure 1a) record ages between 3.4 and 0.5 Ma and were studied by Innocenti et al. (2010). They show similar trace element signatures to the Oligocene to Miocene magmas along Profiles 1 and 2, and Sr isotope ratios between 0.7085 and 0.7094, that decrease with decreasing age. Several studies discussed the petrogenesis of these rocks and suggested that they formed due to back-arc extension or the SW prolongation of the North Anatolian Fault (Fytikas et al., 1984; Innocenti et al., 2010). The subducted slab below the Volos-Evia volcanics is at a depth of 90–100 km, similar to the slab depth below Methana, Aegina, and Milos at the active arc (Halpaap et al., 2018). This implies that this magmatic center is located in a typical position above the slab where mélange melting may cause the formation of magmas. In the W Peloponnese area, the subduction of continental lithosphere lasted until ~10 Ma (Menant, Jolivet, et al., 2016), which is longer than for the Methana segment of the Hellenic subduction. We suggest that the Volos-Evia volcanics represent the NW prolongation of the SAVA (Figure 1a) and that their high-K and high LILE composition correlates with the subduction of continental lithosphere, comparable to the Oligocene to Miocene magmas along Profiles 1 and 2. Due to slow subduction rates during Late Miocene, the subducted continental crust still affected the mantle source of the arc magmas during Pleistocene (Figure 10). Decreasing K contents and $^{87}Sr/^{86}Sr$ from 3.4 to 0.5 Ma (Innocenti et al., 2010) indicate the transition from continental to oceanic subducting lithosphere. Thus, a third profile from Early Miocene magmas in the Chalkidiki area to the young Volos-Evia volcanics documents the migration of arc magmatic activity in the western Aegean (Figure 1a).

6. Conclusions

The ~450 km long approximately linear age-progressive profiles of magmatic centers from NE Greece and NW Turkey to the SAVA reveal a continuous migration of arc magmatic activity perpendicular to the Hellenic Trench, caused by slab rollback during the past 32 Ma. The high compositional variability of the magmas along the profiles can be explained by the transfer of different subducted sediments via heterogeneous mélange diapirs to the mantle source of the arc magmas. We suggest that the generation of Oligocene to Miocene high-K to shoshonitic magmas is caused by relatively low degrees of partial melting

of peridotite-sediment mélange diapirs due to the subduction of continental lithosphere. High $^{87}Sr/^{86}Sr$ in the central Aegean between 20 and 5 Ma reflect a voluminous contribution of subducted clastic material during a period of low subduction rates and underthrusting of continental units. High La/Yb and Th/Yb ratios in mantle-derived magmas in the northern Aegean may be explained by the contribution of metasediments like the Cycladic basement gneisses to the magma source. Increased P/Nd, Ba/La, and Ba/Rb ratios at Maronia, Kassiteres, and Aegina indicate that some of the subducted sediments contained phosphate and barite. Thus, the variable magma compositions of the Aegean reflect the complex subduction of oceanic lithosphere with thick sediment cover as well as continental blocks in the past 30 million years (Menant, Jolivet, et al., 2016; van Hinsbergen et al., 2005).

Data Availability Statement

All new data used in this study can be found in Table S2 and are available on the PANGAEA data repository via Schaarschmidt et al. (2021), https://doi.pangaea.de/10.1594/PANGAEA.915552. All published data used in this study are cited in the Methods section and compiled in Table S1 of the supporting information.

Acknowledgments
The authors would like to thank M. Hertel and M. Regelous for their help with analytical work. The authors gratefully acknowledge the constructive reviews of Horst Marschall and two anonymous reviewers. This research did not receive any specific grant from funding agencies in the public, commercial, or not-for-profit sectors. Open access funding enabled and organized by Projekt DEAL.

References

Abed, A. M. (2013). The eastern Mediterranean phosphorite giants: An interplay between tectonics and upwelling. *GeoArabia, Journal of the Middle East Petroleum Geosciences*, *18*(2), 67–94.

Agostini, S., Doglioni, C., Innocenti, F., Manetti, P., & Tonarini, S. (2010). On the geodynamics of the Aegean rift. *Tectonophysics*, *488*(1–4), 7–21. https://doi.org/10.1016/j.tecto.2009.07.025

Aiuppa, A., Fischer, T. P., Plank, T., Robidoux, P., & Di Napoli, R. (2017). Along-arc, inter-arc and arc-to-arc variations in volcanic gas CO_2/ST ratios reveal dual source of carbon in arc volcanism. *Earth-Science Reviews*, *168*, 24–47. https://doi.org/10.1016/j.earscirev.2017.03.005

Aldanmaz, E., Pearce, J. A., Thirlwall, M. F., & Mitchell, J. G. (2000). Petrogenetic evolution of late Cenozoic, post-collision volcanism in western Anatolia, Turkey. *Journal of Volcanology and Geothermal Research*, *102*, 67–95. https://doi.org/10.1016/S0377-0273(00)00182-7

Altherr, R., & Siebel, W. (2002). I-type plutonism in a continental back-arc setting: Miocene granitoids and monzonites from the central Aegean Sea, Greece. *Contributions to Mineralogy and Petrology*, *143*(4), 397–415. https://doi.org/10.1007/s00410-002-0352-y

Altunkaynak, Ş., & Genç, Ş. C. (2008). Petrogenesis and time-progressive evolution of the Cenozoic continental volcanism in the Biga Peninsula, NW Anatolia (Turkey). *Lithos*, *102*(1–2), 316–340. https://doi.org/10.1016/j.lithos.2007.06.003

Arikas, K., & Voudouris, P. (1998). Hydrothermal alterations and mineralizations of magmatic rocks in the southeastern Rhodope massif. *Acta Vulcanologica*, *10*(2), 353–365.

Baltatzis, E., Esson, J., & Mitropoulos, P. (1992). Geochemical characteristics and petrogenesis of the main granitic intrusions of Greece: An application of trace element discrimination diagrams. *Mineralogical Magazine*, *56*, 487–501. https://doi.org/10.1180/minmag.1992.056.385.05

Barbieri, M., Castorina, F., Masi, U., Tucci, P., Azzaro, E., Kyriakopoulos, K., et al. (1998). Elemental and Sr-Nd isotopic evidence for the origin and geodynamic significance of volcanic rocks from Oxylithos (Central Euboea, Greece). *Bulletin of the Geological Society of Greece*, *32*(3), 251–258.

Behn, M. D., Kelemen, P. B., Hirth, G., Hacker, B. R., & Massonne, H. J. (2011). Diapirs as the source of the sediment signature in arc lavas. *Nature Geoscience*, *4*(9), 641–646. https://doi.org/10.1038/ngeo1214

Bolhar, R., Ring, U., Kemp, A. I. S., Whitehouse, M. J., Weaver, S. D., Woodhead, J. D., et al. (2012). An integrated zircon geochronological and geochemical investigation into the Miocene plutonic evolution of the Cyclades, Aegean Sea, Greece: Part 2-geochemistry. *Contributions to Mineralogy and Petrology*, *164*(6), 915–933. https://doi.org/10.1007/s00410-012-0759-z

Briqueu, L., Javoy, M., Lancelot, J. R., & Tatsumoto, M. (1986). Isotope geochemistry of recent magmatism in the Aegean arc: Sr, Nd, Hf, and O isotopic ratios in the lavas of Milos and Santorini-geodynamic implications. *Earth and Planetary Science Letters*, *80*(1–2), 41–54. https://doi.org/10.1016/0012-821X(86)90018-X

Bröcker, M., Löwen, K., & Rodionov, N. (2014). Unraveling protolith ages of meta-gabbros from Samos and the Attic-Cycladic Crystalline Belt, Greece: Results of a U-Pb zircon and Sr-Nd whole rock study. *Lithos*, *198–199*(1), 234–248. https://doi.org/10.1016/j.lithos.2014.03.029

Brun, J.-P., Faccenna, C., Gueydan, F., Sokoutis, D., Philippon, M., Kydonakis, K., & Gorini, C. (2016). The two-stage Aegean extension, from localized to distributed, a result of slab rollback acceleration. *Canadian Journal of Earth Sciences*, *53*(11), 1142–1157. https://doi.org/10.1139/cjes-2015-0203

Brun, J.-P., & Sokoutis, D. (2010). 45 m.y. of Aegean crust and mantle flow driven by trench retreat. *Geology*, *38*(9), 815–818. https://doi.org/10.1130/G30950.1

Buettner, A., Kleinhanns, I. C., Rufer, D., Hunziker, J. C., & Villa, I. M. (2005). Magma generation at the easternmost section of the Hellenic arc: Hf, Nd, Pb and Sr isotope geochemistry of Nisyros and Yali volcanoes (Greece). *Lithos*, *83*(1–2), 29–46. https://doi.org/10.1016/j.lithos.2005.01.001

Bulle, F., Bröcker, M., Gärtner, C., & Keasling, A. (2010). Geochemistry and geochronology of HP mélanges from Tinos and Andros, cycladic blueschist belt, Greece. *Lithos*, *117*(1–4), 61–81. https://doi.org/10.1016/j.lithos.2010.02.004

Burke, W. H., Denison, R. E., Hetherington, E. A., Koepnick, R. B., Nelson, H. F., & Otto, J. B. (1982). Variation of seawater $^{87}Sr/^{86}Sr$ throughout Phanerozoic time. *Geology*, *10*, 516–519. https://doi.org/10.1130/0091-7613(1982)10<516

Cagnioncle, A., Parmentier, E. M., & Elkins-Tanton, L. T. (2007). Effect of solid flow above a subducting slab on water distribution and melting at convergent plate boundaries. *Journal of Geophysical Research*, *112*, 1–19. https://doi.org/10.1029/2007JB004934

Christofides, G., Eleftheriadis, G., Esson, J., Soldatos, T., Koroneos, A., & Brocker, M. (2000). The evolution of the Samothraki granitic pluton (N. Aegean sea, Greece): Geochronology, chemical and isotopic constraints for AFC modelling. In I. Panayides, C. Xenophontos, & J. Malpas (Eds.), *Paper presented at the third International Conference on the Geology of the Eastern Mediterranean* (pp. 193–209).

Clift, P., & Vannucchi, P. (2004). Controls on tectonic accretion versus erosion in subduction zones: Implications for the origin and recycling of the continental crust. *Reviews of Geophysics*, *42*(2), RG2001. https://doi.org/10.1029/2003RG000127

Codillo, E. A., Le Roux, V., & Marschall, H. R. (2018). Arc-like magmas generated by mélange-peridotite interaction in the mantle wedge. *Nature Communications*, *9*(1), 2864. https://doi.org/10.1038/s41467-018-05313-2

Condamine, P., & Médard, E. (2014). Experimental melting of phlogopite-bearing mantle at 1 GPa: Implications for potassic magmatism. *Earth and Planetary Science Letters*, *397*, 80–92. https://doi.org/10.1016/j.epsl.2014.04.027

Cross, T. A., & Pilger, R. H. (1982). Controls of subduction geometry, location of magmatic arcs, and tectonics of arc and back-arc regions. *GSA Bulletin*, *93*(6), 545–562. https://doi.org/10.1130/0016-7606(1982)93<545:COSGLO>2.0.CO;2

Cruz-Uribe, A. M., Marschall, H. R., Gaetani, G. A., & Le Roux, V. (2018). Generation of alkaline magmas in subduction zones by partial melting of mélange diapirs—An experimental study. *Geology*, *46*(4), 343–346. https://doi.org/10.1130/G39956.1

Delaloye, M., & Bingol, E. (2000). Granitoids from western and northwestern Anatolia: Geochemistry and modeling of geodynamic evolution. *International Geology Review*, *42*(3), 241–268. https://doi.org/10.1080/00206810009465081

Del Moro, A., Innocenti, F., Kyriakopoulos, C., Manetti, P., & Papadopoulos, P. (1988). Tertiary granitoids from Thrace (Northern Greece): Sr isotopic and petrochemical data. *Neues Jahrbuch für Mineralogie-Abhandlungen*, *159*(2), 113–135.

Elburg, M. A., & Smet, I. (2020). Geochemistry of lavas from Aegina and Poros (Aegean Arc, Greece): Distinguishing upper crustal contamination and source contamination in the Saronic Gulf area. *Lithos*, *358–359*, 105416. 10.1016/j.lithos.2020.105416

Elburg, M. A., Smet, I., & De Pelsmaeker, E. (2014). *Influence of source materials and fractionating assemblage on magmatism along the Aegean Arc, and implications for crustal growth* (Vol. 385(1), pp. 137–160). London: Geological Society, Special Publications. https://doi.org/10.1007/s10570-017-1384-910.1144/sp385.1

Elburg, M. A., Smet, I., Van den Haute, P., Vanhaecke, F., Klaver, M., & Andersen, T. (2018). Extreme isotopic variation documents extensional tectonics in arc magmas from Methana, Greece. *Lithos*, *318–319*, 386–398. https://doi.org/10.1016/J.LITHOS.2018.08.029

Elburg, M. A., van Bergen, M. J., & Foden, J. D. (2004). Subducted upper and lower continental crust contributes to magmatism in the collision sector of the Sunda-Banda arc, Indonesia. *Geology*, *32*(1), 41–44. https://doi.org/10.1130/G19941.1

Eleftheriadis, G., Pe-Piper, G., Christofides, G., Soldatos, T., & Esson, J. (1994). K-Ar dating of the Samothraki volcanic rocks, Thrace, northeastern Aegean (Greece). *Bulletin of the Geological Society of Greece*, *30*(1), 205–212.

Emeis, K. C., & Weissert, H. (2009). Tethyan-Mediterranean organic carbon-rich sediments from Mesozoic black shales to sapropels. *Sedimentology*, *56*(1), 247–266. https://doi.org/10.1111/j.1365-3091.2008.01026.x

Ersoy, E. Y., Akal, C., Genç, C., Candan, O., Palmer, M. R., Prelević, D., et al. (2017). U-Pb zircon geochronology of the Paleogene—Neogene volcanism in the NW Anatolia: Its implications for the Late Mesozoic-Cenozoic geodynamic evolution of the Aegean. *Tectonophysics*, *717*, 284–301. https://doi.org/10.1016/j.tecto.2017.08.016

Ersoy, E. Y., & Palmer, M. R. (2013). Eocene-Quaternary magmatic activity in the Aegean: Implications for mantle metasomatism and magma genesis in an evolving orogeny. *Lithos*, *180–181*, 5–24. https://doi.org/10.1016/j.lithos.2013.06.007

Faccenna, C., Becker, T. W., Lucente, F. P., Jolivet, L., & Rossetti, F. (2001). History of subduction and back-arc extension in the Central Mediterranean. *Geophysical Journal International*, *145*(3), 809–820. https://doi.org/10.1046/j.0956-540x.2001.01435.x

Flerit, F., Armijo, R., King, G., & Meyer, B. (2004). The mechanical interaction between the propagating North Anatolian Fault and the back-arc extension in the Aegean. *Earth and Planetary Science Letters*, *224*(3–4), 347–362. https://doi.org/10.1016/j.epsl.2004.05.028

Francalanci, L., Vougioukalakis, G. E., Perini, G., & Manetti, P. (2005). A West-East Traverse along the magmatism of the south Aegean volcanic arc in the light of volcanological, chemical and isotope data. *Developments in Volcanology*, *7*(C), 65–111. https://doi.org/10.1016/S1871-644X(05)80033-6

Francalanci, L., & Zellmer, G. F. (2019). Magma Genesis at the South Aegean Volcanic Arc. *Elements*, *15*(3), 219. https://doi.org/10.2138/gselements.15.3.165

Frei, R. (1995). Evolution of mineralizing fluid in the porphyry copper system of the Skouries Deposit, Northeast Chalkidiki (Greece): Evidence from Combined Pb-Sr and stable isotope data. *Economic Geology*, *90*, 746–762. https://doi.org/10.2113/gsecongeo.90.4.746

Fytikas, M., Giuliani, O., Innocenti, F., Manetti, P., Mazzuoli, R., Peccerillo, A., & Villari, L. (1979). Neogene volcanism of the northern and central Aegean region. *Annales Geologiques Des Pays Helleniques*, *30*, 106–129.

Fytikas, M., Innocenti, F., Kolios, N., Manetti, P., Mazzuoli, R., Poli, G., et al. (1986). Volcanology and petrology of volcanic products from the island of Milos and neighbouring islets. *Journal of Volcanology and Geothermal Research*, *28*, 297–317. https://doi.org/10.1016/0377-0273(86)90028-4

Fytikas, M., Innocenti, F., Manetti, P., Peccerillo, A., Mazzuoli, R., & Villari, L. (1984). *Tertiary to Quaternary evolution of volcanism in the Aegean region*. (Vol. 17(1), pp. 687–699). London: Geological Society, Special Publications. https://doi.org/10.1144/GSL.SP.1984.017.01.55

Gao, J., John, T., Klemd, R., & Xiong, X. (2007). Mobilization of Ti-Nb-Ta during subduction: Evidence from rutile-bearing dehydration segregations and veins hosted in eclogite, Tianshan, NW China. *Geochimica et Cosmochimica Acta*, *71*(20), 4974–4996. https://doi.org/10.1016/j.gca.2007.07.027

Gerya, T. V., & Yuen, D. A. (2003). Rayleigh-Taylor instabilities from hydration and melting propel 'cold plumes' at subduction zones. *Earth and Planetary Science Letters*, *212*(1–2), 47–62. https://doi.org/10.1016/J.CHEMGEO.2016.11.003

Hall, P. S., & Kincaid, C. (2001). Diapiric flow at subduction zones: A recipe for rapid transport. *Science*, *292*(5526), 2472–2475. https://doi.org/10.1126/science.1060488

Halpaap, F., Rondenay, S., & Ottemöller, L. (2018). Seismicity, deformation, and metamorphism in the Western Hellenic subduction zone: New constraints from tomography. *Journal of Geophysical Research: Solid Earth*, *123*(4), 3000–3026. https://doi.org/10.1002/2017JB015154

Hasenclever, J., Morgan, J. P., Hort, M., & Rüpke, L. H. (2011). 2D and 3D numerical models on compositionally buoyant diapirs in the mantle wedge. *Earth and Planetary Science Letters*, *311*(1–2), 53–68. https://doi.org/10.1016/J.EPSL.2011.08.043

Himmerkus, F., Zachariadis, P., Reischmann, T., & Kostopoulos, D. (2012). The basement of the Mount Athos peninsula, northern Greece: Insights from geochemistry and zircon ages. *International Journal of Earth Sciences*, *101*(6), 1467–1485. https://doi.org/10.1007/s00531-011-0644-4

Iglseder, C., Grasemann, B., Schneider, D. A., Petrakakis, K., Miller, C., Klötzli, U. S., et al. (2009). I and S-type plutonism on Serifos (W-Cyclades, Greece). *Tectonophysics*, *473*(1–2), 69–83. https://doi.org/10.1016/j.tecto.2008.09.021

Imamoglu, M. S., Nathan, Y., Çoban, H., Soudry, D., & Glenn, C. (2009). Geochemical, mineralogical and isotopic signatures of the Semikan, West Kasrik "Turkishk" phosphorites from the Derik-Mazidağı-Mardin area, SE Anatolia. *International Journal of Earth Sciences*, *98*(7), 1679–1690. https://doi.org/10.1007/s00531-008-0332-1

Innocenti, F., Agostini, S., Doglioni, C., Manetti, P., & Tonarini, S. (2010). Geodynamic evolution of the Aegean: Constraints from the Plio-Pleistocene volcanism of the Volos-Evia area. *Journal of the Geological Society*, *167*(3), 475–489. https://doi.org/10.1144/0016-76492009-149

Innocenti, F., Kolios, N., Manetti, P., Mazzuoli, R., Peccerillo, G., Rita, F., & Villari, L. (1984). Evolution and geodynamic significance of the tertiary orogenic volcanism in Northeastern Greece. *Bulletin Volcanologique*, *47*(1), 25–37. https://doi.org/10.1007/BF01960538

Innocenti, F., Manetti, P., Peccerillo, A., & Poli, G. (1981). South Aegean volcanic arc: Geochemical variations and geotectonic implications. *Bulletin Volcanologique*, *44*(3), 377–391. https://doi.org/10.1007/BF02600571

Iwamori, H. (1998). Transportation of H_2O and melting in subduction zones. *Earth and Planetary Science Letters*, *160*(1–2), 65–80. https://doi.org/10.1016/S0012-821X(98)00080-6

Jicha, B. R., & Kay, S. M. (2018). Quantifying arc migration and the role of forearc subduction erosion in the central Aleutians. *Journal of Volcanology and Geothermal Research*, *360*, 84–99. https://doi.org/10.1016/j.jvolgeores.2018.06.016

Jolivet, L., & Brun, J.-P. (2010). Cenozoic geodynamic evolution of the Aegean. *International Journal of Earth Sciences*, *99*(1), 109–138. https://doi.org/10.1007/s00531-008-0366-4

Jolivet, L., Faccenna, C., Huet, B., Labrousse, L., Le Pourhiet, L., Lacombe, O., et al. (2013). Aegean tectonics: Strain localisation, slab tearing and trench retreat. *Tectonophysics*, *597–598*, 1–33. https://doi.org/10.1016/j.tecto.2012.06.011

Jones, C. E., Tarney, J., Baker, J. H., & Gerouki, F. (1992). Tertiary granitoids of Rhodope, northern Greece: Magmatism related to extensional collapse of the Hellenic Orogen? *Tectonophysics*, *210*, 295–314. https://doi.org/10.1016/0040-1951(92)90327-3

Juteau, M., Michard, A., & Albarede, F. (1986). The Pb-Sr-Nd isotope geochemistry of some recent circum-Mediterranean granites. *Contributions to Mineralogy and Petrology*, *92*(3), 331–340. https://doi.org/10.1007/BF00572162

Karakonstantis, A., Papadimitriou, P., Millas, C., Spingos, I., Fountoulakis, I., & Kaviris, G. (2019). Tomographic imaging of the NW edge of the Hellenic volcanic arc. *Journal of Seismology*, *23*(5), 995–1016. https://doi.org/10.1007/s10950-019-09849-8

Kirchenbaur, M., Münker, C., Schuth, S., Garbe-Schönberg, D., & Marchev, P. (2012). Tectonomagmatic constraints on the sources of eastern Mediterranean K-rich Lavas. *Journal of Petrology*, *53*(1), 27–65. https://doi.org/10.1093/petrology/egr055

Klaver, M., Davies, G. R., & Vroon, P. Z. (2016). Subslab mantle of African provenance infiltrating the Aegean mantle wedge. *Geology*, *44*(5), 367–370. https://doi.org/10.1130/G37627.1

Klaver, M., Djuly, T., de Graaf, S., Sakes, A., Wijbrans, J., Davies, G., & Vroon, P. (2015). Temporal and spatial variations in provenance of Eastern Mediterranean Sea sediments: Implications for Aegean and Aeolian arc volcanism. *Geochimica et Cosmochimica Acta*, *153*, 149–168. https://doi.org/10.1016/j.gca.2015.01.007

Konzett, J., & Frost, D. J. (2009). The high P-T stability of hydroxyl-apatite in natural and simplified MORB—An experimental study to 15 GPa with implications for transport and storage of phosphorus and halogens in subduction zones. *Journal of Petrology*, *50*(11), 2043–2062. https://doi.org/10.1093/petrology/egp068

Kopf, A. (2003). The Mediterranean Ridge: A mass balance across the fastest growing accretionary complex on Earth. *Journal of Geophysical Research*, *108*(B8), 2372. https://doi.org/10.1029/2001jb000473

Kroll, T., Müller, D., Seifert, T., Herzig, P. M., & Schneider, A. (2002). Petrology and geochemistry of the shoshonite-hosted Skouries porphyry Cu-Au deposit, Chalkidiki, Greece. *Mineralium Deposita*, *37*(1), 137–144. https://doi.org/10.1007/s00126-001-0235-6

Manea, V. C., Leeman, W. P., Gerya, T. V., Manea, M., & Zhu, G. (2014). Subduction of fracture zones controls mantle melting and geochemical signature above slabs. *Nature Communications*, *5*(1), 5095. https://doi.org/10.1038/ncomms6095

Marchev, P., Raicheva, R., Downes, H., Vaselli, O., Chiaradia, M., & Moritz, R. (2004). Compositional diversity of Eocene-Oligocene basaltic magmatism in the Eastern Rhodopes, SE Bulgaria: Implications for genesis and tectonic setting. *Tectonophysics*, *393*(1–4), 301–328. https://doi.org/10.1016/j.tecto.2004.07.045

Marchev, P., Rogers, G., Conrey, R., Quick, J., Vaselli, O., & Raicheva, R. (1998). Paleogene orogenic and alkaline basic magmas in the Rhodope zone: Relationships, nature of magma sources, and role of crustal contamination. *Acta Vulcanologica*, *10*(2), 217–232.

Marschall, H. R., & Schumacher, J. C. (2012). Arc magmas sourced from mélange diapirs in subduction zones. *Nature Geoscience*, *5*(12), 862–867. https://doi.org/10.1038/ngeo1634

Marsh, B. D., & Carmichael, I. S. E. (1974). Benioff zone magmatism. *Journal of Geophysical Research*, *79*(8), 1196–1206. https://doi.org/10.1029/JB079i008p01196

Matsuda, J.-I., Senoh, K., Maruoka, T., Sato, H., & Mitropoulos, P. (1999). K-Ar ages of the Aegean volcanic rocks and their implication for the arc-trench system. *Geochemical Journal*, *33*, 369–377. https://doi.org/10.2343/geochemj.33.369

Mavroudchiev, B., Nedyalkov, R., Eleftheriadis, G., Soldatos, T., & Christofides, G. (1993). Tertiary plutonic rocks from East Rhodope in Bulgaria and Greece. *Bulletin of the Geological Society of Greece*, *28*(2), 643–660.

McDade, P., Blundy, J. D., & Wood, B. J. (2003). Trace element partitioning between mantle wedge peridotite and hydrous MgO-rich melt. *American Mineralogist*, *88*(11–12), 1825–1831. https://doi.org/10.2138/am-2003-11-1225

McGary, R. S., Evans, R. L., Wannamaker, P. E., Elsenbeck, J., & Rondenay, S. (2014). Pathway from subducting slab to surface for melt and fluids beneath Mount Rainier. *Nature*, *511*(7509), 338–340. https://doi.org/10.1038/nature13493

McGrath, A., Stouraiti, C., & Windley, B. (2017). Geochemistry of mylonitic gneisses from the Cycladic Basement Unit (Paros and Serifos, Aegean Sea): Implications for protoliths of the high-grade gneisses. *International Journal of Earth Sciences*, *106*(6), 2067–2089. https://doi.org/10.1007/s00531-016-1414-0

Melfos, V., Vavelidis, M., Christofides, G., & Seidel, E. (2002). Origin and evolution of the Tertiary Maronia porphyry copper-molybdenum deposit, Thrace, Greece. *Mineralium Deposita*, *37*(6–7), 648–668. https://doi.org/10.1007/s00126-002-0277-4

Menant, A., Jolivet, L., & Vrielynck, B. (2016). Kinematic reconstructions and magmatic evolution illuminating crustal and mantle dynamics of the eastern Mediterranean region since the late Cretaceous. *Tectonophysics*, *675*, 103–140. https://doi.org/10.1016/j.tecto.2016.03.007

Menant, A., Sternai, P., Jolivet, L., Guillou-Frottier, L., & Gerya, T. V. (2016). 3D numerical modeling of mantle flow, crustal dynamics and magma genesis associated with slab roll-back and tearing: The eastern Mediterranean case. *Earth and Planetary Science Letters*, *442*, 93–107. https://doi.org/10.1016/j.epsl.2016.03.002

Mitropoulos, P., Tarney, J., Saunders, A. D., & Marsh, N. G. (1987). Petrogenesis of Cenozoic volcanic rocks from the Aegean island arc. *Journal of Volcanology and Geothermal Research*, *32*, 177–193.

Nicholls, A. I. A., & Ringwood, A. E. (1973). Effect of water on olivine stability in tholeiites and the production of silica-saturated magmas in the island-arc environment. *The University of Chicago Press Journal*, *81*(3), 285–300. https://doi.org/10.1086/627871

Notholt, A. J. G. (1985). Phosphorite resources in the Mediterranean (Tethyan) phosphogenic province: A progress report. *Sciences Geologiques Memoire*, *77*, 9–21.

Papadopoulou, L., Christofides, G., Bröcker, M., Koroneos, A., Soldatos, T., & Eleftheriadis, G. (2001). Petrology, geochemistry and isotopic characteristics of the shoshonitic plutonic rocks from Maronia area, West Thrace, Greece. *Bulletin of the Geological Society of Greece*, *34*(3), 967–976. https://doi.org/10.12681/bgsg.17129

Papadopoulou, L., Christofides, G., Koroneos, A., Soldatos, T., & Eleftheriadis, G. (2004). Evolution and origin of the Maronia Pluton, Thrace, Greece. *Bulletin of the Geological Society of Greece*, *36*, 568–577. https://doi.org/10.12681/bgsg.16754

Paul, A., Karabulut, H., Mutlu, A. K., & Salaün, G. (2014). A comprehensive and densely sampled map of shear-wave azimuthal anisotropy in the Aegean-Anatolia region. *Earth and Planetary Science Letters*, *389*, 14–22. https://doi.org/10.1016/j.epsl.2013.12.019

Pearce, F. D., Rondenay, S., Sachpazi, M., Charalampakis, M., & Royden, L. H. (2012). Seismic investigation of the transition from continental to oceanic subduction along the western Hellenic Subduction Zone. *Journal of Geophysical Research: Solid Earth*, *117*, B07306. https://doi.org/10.1029/2011JB009023

Pearce, J. A., & Stern, R. J. (2006). Origin of back-arc basin magmas: Trace element and isotope perspectives. *Geophysical Monograph Series*, *166*, 63–86. https://doi.org/10.1029/166GM06

Peccerillo, A., De Astis, G., Faraone, D., Forni, F., & Frezzotti, M. L. (2013). Compositional variations of magmas in the aeolian arc: Implications for petrogenesis and geodynamics. *Geological Society Memoir*, *37*(1), 491–510. https://doi.org/10.1144/M37.15

Peccerillo, A., & Taylor, S. R. (1976). Geochemistry of eocene calc-alkaline volcanic rocks from the Kastamonu area, Northern Turkey. *Contributions to Mineralogy and Petrology*, *58*(1), 63–81. https://doi.org/10.1007/BF00384745

Pe-Piper, G. (1991). Magnesian andesites from the island of Skyros, Greece: Geochemistry and regional significance. *Geological Magazine*, *128*(6), 585–593. https://doi.org/10.1017/S0016756800019701

Pe-Piper, G., & Piper, D. J. W. (1992). Geochemical variation with time in the Cenozoic high-k volcanic rocks of the island of Lesbos, Greece: Significance for shoshonite petrogenesis. *Journal of Volcanology and Geothermal Research*, *53*(1–4), 371–387. https://doi.org/10.1016/0377-0273(92)90092-R

Pe-Piper, G., & Piper, D. J. W. (1994). Miocene magnesian andesites and dacites, Evia, Greece: Adakites associated with subducting slab detachment and extension. *Lithos*, *31*(3–4), 125–140. https://doi.org/10.1016/0024-4937(94)90004-3

Pe-Piper, G., & Piper, D. J. W. (2001). Late Cenozoic, post-collisional Aegean igneous rocks: Nd, Pb and Sr isotopic constraints on petrogenetic and tectonic models. *Geological Magazine*, *138*(6), 653–668. https://doi.org/10.1017/S0016756801005957

Pe-Piper, G., & Piper, D. J. W. (2006). *Unique features of the Cenozoic igneous rocks of Greece*. (Vol. 409, p. 259). Geological Society of America Special Paper.

Pe-Piper, G., & Piper, D. J. W. (2013). The effect of changing regional tectonics on an arc volcano: Methana, Greece. *Journal of Volcanology and Geothermal Research*, *260*, 146–163. https://doi.org/10.1016/j.jvolgeores.2013.05.011

Pe-Piper, G., Piper, D. J. W., Kotopouli, C. N., & Panagos, A. G. (1994). *Neogene volcanoes of Chios, Greece: The relative importance of subduction and back-arc extension*. (Vol. 81, pp. 213–231). Geological Society Special Publication. https://doi.org/10.1144/GSL.SP.1994.081.01.12

Pe-Piper, G., Piper, D. J. W., Koukouvelas, I., Dolansky, L. M., & Kokkalas, S. (2009). Postorogenic shoshonitic rocks and their origin by melting underplated basalts: The Miocene of Limnos, Greece. *Bulletin of the Geological Society of America*, *121*(1–2), 39–54. https://doi.org/10.1130/B26317.1

Pe-Piper, G., Piper, D. J. W., & Matarangas, D. (2002). Regional implications of geochemistry and style of emplacement of Miocene I-type diorite and granite, Delos, Cyclades, Greece. *Lithos*, *60*(1–2), 47–66. https://doi.org/10.1016/S0024-4937(01)00068-8

Pe-Piper, G., Piper, D. J. W., & Reynolds, P. H. (1983). Paleomagnetic stratigraphy and radiometric dating of the Pliocene volcanic rocks of Aegina, Greece. *Bulletin Volcanologique*, *46*(1), 1–7. https://doi.org/10.1007/BF02598241

Pe-Piper, G., Zhang, Y., Piper, D. J. W., & Prelević, D. (2014). Relationship of Mediterranean type lamproites to large shoshonite volcanoes, Miocene of Lesbos, NE Aegean Sea. *Lithos*, *184–187*, 281–299. https://doi.org/10.1016/j.lithos.2013.11.004

Perkins, R. J., Cooper, F. J., Condon, D. J., Tattitch, B. C., & Naden, J. (2018). Post-collisional Cenozoic extension in the northern Aegean: The high-K to shoshonitic intrusive rocks of the Maronia Magmatic Corridor, northeastern Greece. *Lithosphere*, *10*(5), 582–601. https://doi.org/10.1130/l730.1

Plank, T., & Langmuir, C. H. (1993). Tracing trace elements from sediment input to volcanic output at subduction zones. *Nature*, *362*(6422), 739–743. https://doi.org/10.1038/362739a0

Plank, T., & Langmuir, C. H. (1998). The chemical composition of subducting sediment and its consequences for the crust and mantle. *Chemical Geology*, *145*(3–4), 325–394. https://doi.org/10.1016/S0009-2541(97)00150-2

Qian, Q., & Hermann, J. (2013). Partial melting of lower crust at 10–15 kbar: Constraints on adakite and TTG formation. *Contributions to Mineralogy and Petrology*, *165*(6), 1195–1224. https://doi.org/10.1007/s00410-013-0854-9

Rogers, N. W., & Setterfield, T. N. (1994). Potassium and incompatible-element enrichment in shoshonitic lavas from the Tavua volcano, Fiji. *Chemical Geology*, *118*, 43–62. https://doi.org/10.1016/0009-2541(94)90169-4

Royden, L. H. (1993). Evolution of retreating subduction boundaries formed during continental 1080 collision. *Tectonics*, *12*(3), 629–638. https://doi.org/10.1029/92TC02641

Royden, L. H., & Faccenna, C. (2018). Subduction orogeny and the late Cenozoic evolution of the Mediterranean arcs. *Annual Review of Earth and Planetary Sciences*, *46*, 261–289. https://doi.org/10.1146/annurev-earth-060115-012419

Royden, L. H., & Papanikolaou, D. J. (2011). Slab segmentation and late Cenozoic disruption of the Hellenic arc. *Geochemistry, Geophysics, Geosystems*, *12*(3), 1–24. https://doi.org/10.1029/2010GC003280

Roy, M., Jordan, T. H., & Pederson, J. (2009). Colorado Plateau magmatism and uplift by warming of heterogeneous lithosphere. *Nature*, *459*(7249), 978–982. https://doi.org/10.1038/nature08052

Sachpazi, M., Laigle, M., Charalampakis, M., Diaz, J., Kissling, E., Gesret, A., et al. (2016). Segmented Hellenic slab rollback driving Aegean deformation and seismicity. *Geophysical Research Letters*, *43*(2), 651–658. https://doi.org/10.1002/2015GL066818

Schaarschmidt, A., Klemd, R., Regelous, M., Voudouris, P. C., Melfos, V., & Haase, K. M. (2021). The formation of shoshonitic magma and its relationship to porphyry-type mineralization: The Maronia pluton in NE Greece. *Lithos*, *380–381*, 105911. https://doi.org/10.1016/j.lithos.2020.105911

Schmidt, M. W., & Jagoutz, O. (2017). The global systematics of primitive arc melts. *Geochemistry, Geophysics, Geosystems*, *18*(8), 2817–2854. https://doi.org/10.1002/2016GC006699

Seyitoğlu, G., & Scott, B. C. (1992). Late Cenozoic volcanic evolution of the northeastern Aegean region. *Journal of Volcanology and Geothermal Research*, *54*(1–2), 157–176. https://doi.org/10.1016/0377-0273(92)90121-S

Skarpelis, N., Tsikouras, B., & Pe-Piper, G. (2008). The Miocene igneous rocks in the Basal Unit of Lavrion (SE Attica, Greece): Petrology and geodynamic implications. *Geological Magazine*, *145*(1), 1–15. https://doi.org/10.1017/s0016756807003949

Sodoudi, F., Kind, R., Hatzfeld, D., Priestley, K., Hanka, W., Wylegalla, K., et al. (2006). Lithospheric structure of the Aegean obtained from P and S receiver functions. *Journal of Geophysical Research*, *111*(12), 1–23. https://doi.org/10.1029/2005JB003932

Spandler, C., Mavrogenes, J., & Hermann, J. (2007). Experimental constraints on element mobility from subducted sediments using high-P synthetic fluid/melt inclusions. *Chemical Geology*, *239*(3–4), 228–249. https://doi.org/10.1016/j.chemgeo.2006.10.005

Spiegelman, M., & McKenzie, D. (1987). Simple 2-D models for melt extraction at mid-ocean ridges and island arcs. *Earth and Planetary Science Letters*, *83*(1–4), 137–152. https://doi.org/10.1016/0012-821X(87)90057-4

Stouraiti, C., Baziotis, I., Asimow, P. D., & Downes, H. (2018). *Geochemistry of the Serifos calc-alkaline granodiorite pluton, Greece: Constraining the crust and mantle contributions to I-type granitoids. International Journal of Earth Sciences* (Vol. 107). Springer Berlin Heidelberg. https://doi.org/10.1007/s00531-017-1565-7

Stouraiti, C., Mitropoulos, P., Tarney, J., Barreiro, B., McGrath, A. M., & Baltatzis, E. (2010). Geochemistry and petrogenesis of late Miocene granitoids, Cyclades, southern Aegean: Nature of source components. *Lithos*, *114*(3–4), 337–352. https://doi.org/10.1016/j.lithos.2009.09.010

Stouraiti, C., Pantziris, I., Vasilatos, C., Kanellopoulos, C., Mitropoulos, P., Pomonis, P., et al. (2017). Ophiolitic remnants from the upper and intermediate structural unit of the Attic-Cycladic Crystalline Belt (Aegean, Greece): Fingerprinting geochemical affinities of magmatic precursors. *Geosciences*, *7*(1), 14. https://doi.org/10.3390/geosciences7010014

Sun, S. S., & McDonough, W. F. (1989). *Chemical and isotopic systematics of oceanic basalts: Implications for mantle composition and processes*. (Vol. 42, pp. 313–345). London: Geological Society, Special Publications. https://doi.org/10.1144/GSL.SP.1989.042.01.19

Tamura, Y., Tatsumi, Y., Zhao, D., Kido, Y., & Shukuno, H. (2002). Hot fingers in the mantle wedge: New insights into magma genesis in subduction zones. *Earth and Planetary Science Letters*, *197*(1–2), 105–116. https://doi.org/10.1016/S0012-821X(02)00465-X

Tatsumi, Y. (1986). Formation of the volcanic front in subduction zones. *Geophysical Research Letters*, *13*(8), 717–720. https://doi.org/10.1029/GL013i008p00717

Tesauro, M., Kaban, M. K., & Cloetingh, S. A. P. L. (2009). A new thermal and rheological model of the European lithosphere. *Tectonophysics*, *476*(3–4), 478–495. https://doi.org/10.1016/j.tecto.2009.07.022

Uzel, B., Kuiper, K., Sözbilir, H., Kaymakci, N., Langereis, C. G., & Boehm, K. (2020). Miocene geochronology and stratigraphy of western Anatolia: Insights from new Ar/Ar dataset. *Lithos*, *352–353*. https://doi.org/10.1016/j.lithos.2019.105305

van Hinsbergen, D. J. J., Hafkenscheid, E., Spakman, W., Meulenkamp, J. E., & Wortel, R. (2005). Nappe stacking resulting from subduction of oceanic and continental lithosphere below Greece. *Geology*, *33*(4), 325–328. https://doi.org/10.1130/G20878.1

Vlahou, M., Christofides, G., Eleftheriadis, G., Pinarelli, L., & Koroneos, A. (2006). Tertiary volcanic rocks from Samothraki island (north Aegean, Greece): Sr and Nd isotope constraints on their evolution. *Geological Society of America Special Papers*, *409*, 283–304. https://doi.org/10.1130/2006.2409(15

Wehausen, R., & Brumsack, H. J. (1999). Cyclic variations in the chemical composition of eastern Mediterranean Pliocene sediments: A key for understanding sapropel formation. *Marine Geology*, *153*(1–4), 161–176. https://doi.org/10.1016/S0025-3227(98)00083-8

Wei, W., Zhao, D., Wei, F., Bai, X., & Xu, J. (2019). Mantle dynamics of the eastern Mediterranean and Middle East: Constraints from P-wave anisotropic tomography. *Geochemistry, Geophysics, Geosystems*, *20*(10), 4505–4530. https://doi.org/10.1029/2019GC008512

Woelki, D., Haase, K. M., Schoenhofen, M. V., Beier, C., Regelous, M., Krumm, S. H., & Günther, T. (2018). Evidence for melting of subducting carbonate-rich sediments in the western Aegean Arc. *Chemical Geology*, *483*, 463–473. https://doi.org/10.1016/j.chemgeo.2018.03.014

Workman, R. K., & Hart, S. R. (2005). Major and trace element composition of the Depleted MORB Mantle (DMM). *Earth and Planetary Science Letters*, *231*(1–2), 53–72. https://doi.org/10.1016/j.epsl.2004.12.005

Wortel, M. J. R., & Spakman, W. (2000). Subduction and slab detachment in the Mediterranean-Carpathian region. *Science*, *290*(5498), 1910–1917. https://doi.org/10.1126/science.290.5498.1910

Yigit, O. (2012). A prospective sector in the Tethyan Metallogenic Belt: Geology and geochronology of mineral deposits in the Biga Peninsula, NW Turkey. *Ore Geology Reviews*, *46*, 118–148. https://doi.org/10.1016/j.oregeorev.2011.09.015

Zhang, Z., Xiao, X., Wang, J., Wang, Y., & Kusky, T. M. (2008). Post-collisional Plio-Pleistocene shoshonitic volcanism in the western Kunlun Mountains, NW China: Geochemical constraints on mantle source characteristics and petrogenesis. *Journal of Asian Earth Sciences*, *31*(4–6), 379–403. https://doi.org/10.1016/j.jseaes.2007.06.003

References From the Supporting Information

Blundy, J. D., Robinson, J. A. C., & Wood, B. J. (1998). Heavy REE are compatible in clinopyroxene on the spinel lherzolite solidus. *Earth and Planetary Science Letters*, *160*(3–4), 493–504. https://doi.org/10.1016/S0012-821X(98)00106-X

Buettner, A., Kleinhanns, I. C., Rufer, D., Hunziker, J. C., & Villa, I. M. (2005). Magma generation at the easternmost section of the Hellenic arc: Hf, Nd, Pb and Sr isotope geochemistry of Nisyros and Yali volcanoes (Greece). *Lithos*, *83*(1–2), 29–46. https://doi.org/10.1016/j.lithos.2005.01.001

Freund, S., Beier, C., Krumm, S., & Haase, K. M. (2013). Oxygen isotope evidence for the formation of andesitic-dacitic magmas from the fast-spreading Pacific-Antarctic Rise by assimilation-fractional crystallisation. *Chemical Geology*, *347*, 271–283. https://doi.org/10.1016/j.chemgeo.2013.04.013

Govindaraju, K. (1994). Compilation of working values and sample description for 383 Geostandards. *Geostandards Newsletter*, *18*, 1–158. https://doi.org/10.1046/j.1365-2494.1998.53202081.x-i1

Haase, K. M., Beier, C., Regelous, M., Rapprich, V., & Renno, A. (2017). Spatial variability of source composition and petrogenesis in rift and rift flank alkaline lavas from the Eger Rift, Central Europe. *Chemical Geology*, *455*, 304–314. https://doi.org/10.1016/J.CHEMGEO.2016.11.003

Hermann, J., & Rubatto, D. (2009). Accessory phase control on the trace element signature of sediment melts in subduction zones. *Chemical Geology*, *265*(3–4), 512–526. https://doi.org/10.1016/j.chemgeo.2009.05.018

Klaver, M., Djuly, T., de Graaf, S., Sakes, A., Wijbrans, J., Davies, G., & Vroon, P. (2015). Temporal and spatial variations in provenance of Eastern Mediterranean Sea sediments: Implications for Aegean and Aeolian arc volcanism. *Geochimica et Cosmochimica Acta*, *153*, 149–168. https://doi.org/10.1016/j.gca.2015.01.007

McDade, P., Blundy, J. D., & Wood, B. J. (2003). Trace element partitioning on the Tinaquillo solidus at 1.5 GPa. *Physics of the Earth and Planetary Interiors*, *139*(1–2), 129–147. https://doi.org/10.1016/S0031-9201(03)00149-3

McGrath, A., Stouraiti, C., & Windley, B. (2017). Geochemistry of mylonitic gneisses from the Cycladic Basement Unit (Paros and Serifos, Aegean Sea): Implications for protoliths of the high-grade gneisses. *International Journal of Earth Sciences*, *106*(6), 2067–2089. https://doi.org/10.1007/s00531-016-1414-0

Nielsen, S. G., & Marschall, H. R. (2017). Geochemical evidence for mélange melting in global arcs. *Science Advances*, *3*(4), 1–7. https://doi.org/10.1126/sciadv.1602402

Wood, B. J., Blundy, J. D., & Robinson, J. A. C. (1999). The role of clinopyroxene in generating U-series disequilibrium during mantle melting. *Geochimica et Cosmochimica Acta*, *63*(10), 1613–1620. https://doi.org/10.1016/S0016-7037(98)00302-0

Workman, R. K., & Hart, S. R. (2005). Major and trace element composition of the Depleted MORB Mantle (DMM). *Earth and Planetary Science Letters*, *231*(1–2), 53–72. https://doi.org/10.1016/j.epsl.2004.12.005